

⁴European Commission, Joint Research Centre, Institute for Environment and Sustainability, Ispra (VA), Italy

⁵INERIS, Verneuil-en-Halatte, France

⁶NILU – Norwegian Institute for Air Research, Kjeller, Norway

⁷Department of Physics, University of Helsinki, Helsinki, Finland

⁸Institute of Environmental Assessment and Water Research (IDAEA-CSIC), Barcelona, Spain

⁹Centre for Energy, Environment and Technology Research (CIEMAT), Department of the Environment, Madrid, Spain

¹⁰Proambiente S.c.r.l., CNR Research Area, Bologna, Italy

¹¹Aerodyne Research, Inc., Billerica, Massachusetts, USA

¹²TOFWERK AG, Thun, Switzerland

¹³Deutscher Wetterdienst, Meteorologisches Observatorium Hohenpeißenberg, Hohenpeißenberg, Germany

¹⁴Environmental Research Group, MRC-HPA Centre for Environment and Health, King's College London, London, UK

¹⁵Leibniz Institute for Tropospheric Research, Leipzig, Germany

¹⁶Aerosol d.o.o., Ljubljana, Slovenia

¹⁷School of Physics and Centre for Climate and Air Pollution Studies, Ryan Institute, National University of Ireland Galway, Galway, Ireland

¹⁸ENEA-National Agency for New Technologies, Energy and Sustainable Economic Development, Bologna, Italy

¹⁹The Cyprus Institute, Environment Energy and Water Research Center, Nicosia, Cyprus

Received: 24 December 2014 – Accepted: 19 January 2015 – Published: 4 February 2015

Correspondence to: A. S. H. Prévôt (andre.prevot@psi.ch)

Published by Copernicus Publications on behalf of the European Geosciences Union.

Intercomparison of ME-2 organic source apportionment

R. Fröhlich et al.

Title Page

Abstract

Introduction

Conclusions

References

Tables

Figures



Back

Close

Full Screen / Esc

Printer-friendly Version

Interactive Discussion



Abstract

Chemically resolved atmospheric aerosol data sets from the largest intercomparison of the Aerodyne aerosol chemical speciation monitors (ACSM) performed to date were collected at the French atmospheric supersite SIRTA. In total 13 quadrupole ACSMs (Q-ACSM) from the European ACTRIS ACSM network, one time-of-flight ACSM (ToF-ACSM), and one high-resolution ToF aerosol mass spectrometer (AMS) were operated in parallel for about three weeks in November and December 2013. Part 1 of this study reports on the accuracy and precision of the instruments for all the measured species. In this work we report on the intercomparison of organic components and the results from factor analysis source apportionment by positive matrix factorisation (PMF) utilising the multilinear engine 2 (ME-2). Except for the organic contribution of m/z 44 to the total organics (f44), which varied by factors between 0.6 and 1.3 compared to the mean, the peaks in the organic mass spectra were similar among instruments. The m/z 44 differences in the spectra resulted in a variable f44 in the source profiles extracted by ME-2, but had only a minor influence on the extracted mass contributions of the sources. The presented source apportionment yielded four factors for all 15 instruments: hydrocarbon-like organic aerosol (HOA), cooking-related organic aerosol (COA), biomass burning-related organic aerosol (BBOA) and secondary oxygenated organic aerosol (OOA). Individual application and optimisation of the ME-2 boundary conditions (profile constraints) are discussed together with the investigation of the influence of alternative anchors (reference profiles). A comparison of the ME-2 source apportionment output of all 15 instruments resulted in relative SD from the mean between 13.7 and 22.7 % of the source's average mass contribution depending on the factors (HOA: 14.3 ± 2.2 %, COA: 15.0 ± 3.4 %, OOA: 41.5 ± 5.7 %, BBOA: 29.3 ± 5.0 %). Factors which tend to be subject to minor factor mixing (in this case COA) have higher relative uncertainties than factors which are recognised more readily like the OOA. Averaged over all factors and instruments the relative first SD from the mean of a source extracted with ME-2 was 17.2 %.

Intercomparison of ME-2 organic source apportionment

R. Fröhlich et al.

Title Page

Abstract

Introduction

Conclusions

References

Tables

Figures



Back

Close

Full Screen / Esc

Printer-friendly Version

Interactive Discussion



1 Introduction

Measurements have shown that organic compounds constitute a major fraction of the total particulate matter (PM) all around the world (20–90% of the submicron aerosol mass according to Kanakidou et al., 2005). Elevated concentrations of organic aerosols due to anthropogenic activities are a major contributor to the predominantly adverse effects of aerosols on climate (Lohmann and Feichter, 2005; Stevens and Feingold, 2009; Boucher et al., 2013; Carslaw et al., 2013), weather extremes (Wang et al., 2014a, b), Earth's ecosystem (Mercado et al., 2009; Carslaw et al., 2010; Mahowald, 2011) or on human health (Seaton et al., 1995; Laden et al., 2000; Cohen et al., 2005; Pope and Dockery, 2006). According to recent estimates of the global burden of disease up to 3.6 million (Lim et al., 2013) of the about 56 million annual deaths (Mathers et al., 2005) were connected to ambient particulate air pollution in the year 2010. These numbers underline the importance of detailed knowledge about the sources of ambient aerosols to be able to efficiently reduce air pollution levels.

Positive matrix factorisation (PMF), a statistical factor analysis algorithm developed by Paatero and Tapper (1994) and Paatero (1997), is a widely and successfully used approach to simplify interpretation of complex data sets by representing measurements as a linear combination of static factor profiles and their time-dependent intensities (Lanz et al., 2007, 2010; Ulbrich et al., 2009; Crippa et al., 2014). The multilinear engine implementation (ME-2, Paatero, 1999) allows for the introduction of additional constraints (e.g. external factor profiles) to the algorithm. The algorithm has been heavily used for source identification and quantification with organic mass spectra measured by the Aerodyne aerosol mass spectrometer (AMS Jayne et al., 2000; Drewnick et al., 2005; DeCarlo et al., 2006) and the related aerosol chemical speciation monitor (ACSM, Ng et al., 2011c; Fröhlich et al., 2013). Typically, the organic fraction of PM can be split up in primary (POA) and secondary organic aerosol (SOA). Origin and precursors of the SOA, which often can be separated according to volatility into a more oxidised (low-volatile LV-OOA) and a less oxidised fraction (“semi”-volatile SV-OOA)

AMTD

8, 1559–1613, 2015

Intercomparison of ME-2 organic source apportionment

R. Fröhlich et al.

Title Page

Abstract

Introduction

Conclusions

References

Tables

Figures



Back

Close

Full Screen / Esc

Printer-friendly Version

Interactive Discussion



2 Methodology and instrument description

The 15 Aerodyne mass spectrometers, which were provided by the co-authoring institutions (see Table S1 in the Supplement) will be denoted herein as #1–#13 (Q-ACSMs), ToF (ToF-ACSM) and HR(-AMS) (HR-ToF-AMS). Overviews of wintertime aerosol sources and composition in the Paris region can be found in Crippa et al. (2013a) and Bressi et al. (2014). The data sets were recorded during the ACTRIS ACSM intercomparison campaign taking place during three weeks in November and December 2013 at the SIRTAs (Site Instrumental de Recherche par Télédétection Atmosphérique) station of the LSCE (Laboratoire des sciences du climat et l'environnement) in Gif-sur-Yvette, in the region of Paris (France). Detailed results of the intercomparison can be found in part I of this study from Cretn et al. (2015). For this intercomparison study data between 16 November and 1 December were considered.

2.1 Site description

SIRTA is a well-established atmospheric observatory in the vicinity of the French megacity Paris. The measurement site is located on the plateau of Saclay on the campus of CEA (French Alternative Energies and Atomic Energy Commission) at “Orme des Merisiers” (48.709° N, 2.149° E, 163 m a.s.l.). Being approximately 20 km south-west of the city centre of Paris, the station is classified as regional background, surrounded mainly by agricultural fields, forests, small villages and other research facilities. The closest major road is located about 2 km north-east.

All 15 instruments were located in the same laboratory, distributed to five separate PM_{2.5} inlets on the roof of the building. A suite of additional aerosol and gas phase instruments (e.g. Particle-Into-Liquid-Sampler coupled to an ion chromatograph (PILS-IC), proton-transfer-reaction mass spectrometer (PTR-MS), filter sampling, aethalometer, nephelometer, scanning mobility particle sizer (SMPS), optical particle counter (OPC), tapered element oscillating microbalances and filter dynamics measurement system (TEOM-FDMS) – for a complete list and description of the inlets and collocated

AMTD

8, 1559–1613, 2015

Intercomparison of ME-2 organic source apportionment

R. Fröhlich et al.

Title Page

Abstract

Introduction

Conclusions

References

Tables

Figures

◀

▶

◀

▶

Back

Close

Full Screen / Esc

Printer-friendly Version

Interactive Discussion



data analysis. The fragmentation table was adjusted according to recommendations (Aiken et al., 2008) in order to take into account air interferences and the water fragmentation pattern.

2.3 Aethalometer, NO_x analyser and PTR-MS

In the context of this manuscript, data from various external measurements, namely an aethalometer, a NO_x analyser and a PTR-MS were used to validate factors found by the ME-2 source apportionment. The Magee Scientific Aethalometer model AE33 (Drinovec et al., 2014, Aerosol d.o.o., Ljubljana, Slovenia) measures black carbon (BC) aerosol by collecting aerosol on a filter and determining the light absorption at seven different wavelengths (Hansen et al., 1984). Potential sample loading artefacts detailed in Collaud Coen et al. (2010) are automatically compensated for according to the procedures described in Drinovec et al. (2014). The absorption coefficient b_{abs} depends on the wavelength λ and the Ångström exponent α_i , following the relationship

$$b_{\text{abs}} \propto \lambda^{-\alpha_i}. \quad (1)$$

By exploiting the fact that the wavelength dependence, i.e. the Ångström exponent is source-specific (Sandradewi et al., 2008), the measured BC can be separated into BC from wood burning (BC_{wb}) and BC from fossil fuel combustion (BC_{ff}). To this end a system of four equations has to be solved.

$$\frac{b_{\text{abs}}(\lambda_1)_{\text{ff}}}{b_{\text{abs}}(\lambda_2)_{\text{ff}}} = \left(\frac{\lambda_1}{\lambda_2}\right)^{-\alpha_{\text{ff}}} \quad (2)$$

$$\frac{b_{\text{abs}}(\lambda_1)_{\text{wb}}}{b_{\text{abs}}(\lambda_2)_{\text{wb}}} = \left(\frac{\lambda_1}{\lambda_2}\right)^{-\alpha_{\text{wb}}} \quad (3)$$

$$b_{\text{abs}}(\lambda_1)_{\text{tot}} = b_{\text{abs}}(\lambda_1)_{\text{ff}} + b_{\text{abs}}(\lambda_1)_{\text{wb}} \quad (4a)$$

$$b_{\text{abs}}(\lambda_2)_{\text{tot}} = b_{\text{abs}}(\lambda_2)_{\text{ff}} + b_{\text{abs}}(\lambda_2)_{\text{wb}} \quad (4b)$$

Intercomparison of ME-2 organic source apportionment

R. Fröhlich et al.

Title Page

Abstract

Introduction

Conclusions

References

Tables

Figures



Back

Close

Full Screen / Esc

Printer-friendly Version

Interactive Discussion



ing away from the unconstrained solution typically leads to an increase in Q . The magnitude of this increase of Q is used in order to remove solutions whose rotations are not a mathematically adequate representation of the input dataset. All factor analyses presented in this study were performed in the robust mode (Paatero, 1997).

5 Initialisation of the ME-2 engine and analysis of the results was performed using the source finder tool (SoFi v4.6, <http://psi.ch/HGdP>, Canonaco et al., 2013) package for Igor Pro (WaveMetrics Inc., Lake Oswego, Oregon).

2.5 Model input and data preparation

As an input, the ME-2 algorithm requires the organic data matrix, the associated error matrix, and the corresponding time and mass-to-charge (m/z) axis. For each instrument the input data was created up to m/z 100 and individually cleaned up. Bad data points were identified by standard diagnostics (airbeam signal, inlet pressure, voltage settings, etc.). A uniform CE = 0.5 and a uniform organics RIE_{org} = 1.4 were used for all data sets. The corresponding ionisation efficiency (IE) or, more accurately for the Q-ACSMs, the response factor (RF) calibration values were determined during the first week of the intercomparison study on site (Crenn et al., 2015) and can be found in Table S2. Q-ACSM data was corrected for a decrease in ion transmission at high m/z (≥ 55) according to a standard curve obtained by Ng et al. (2011c). For further discussion and recent software updates concerning the RIT calculation for PMF matrices refer to the discussion in the Supplement. To correct for the decay of the detector amplification the airbeam N₂ signal at m/z 28 was used (reference value: 1×10^{-7} A) maintaining the detectors at gain values of around 20 000.

25 The ToF-ACSM data set exhibited an unusual (exponentially decaying) drift in addition to the drift of the airbeam signals, visible in the always present background signals like the one of stable tungsten isotopes (originating from the ioniser filament). From the largest signals in the background (m/z 105, 130, 132, 182 and 221) a correction function was deduced and applied to the data set. This drift is attributed to transient effects in the electronics occurring after the replacement of the electron multiplier.

Intercomparison of ME-2 organic source apportionment

R. Fröhlich et al.

Title Page

Abstract

Introduction

Conclusions

References

Tables

Figures



Back

Close

Full Screen / Esc

Printer-friendly Version

Interactive Discussion



Intercomparison of ME-2 organic source apportionment

R. Fröhlich et al.

Title Page

Abstract

Introduction

Conclusions

References

Tables

Figures



Back

Close

Full Screen / Esc

Printer-friendly Version

Interactive Discussion



displayed as black line with the interquartile range (IQR) (25–75 percentile) shaded in red and the 10–90 percentile range shaded in grey. The corrected ToF-ACSM time series is shown in green and the AMS in pink. Correlations of ToF-ACSM and AMS with the median of the Q-ACSMs is shown in the two inset graphs. Good qualitative and quantitative agreement between all 15 aerosol mass spectrometers was achieved ($R^2 = 0.82$ – 0.99 , slope = 0.70 – 1.37 , see Crenn et al. (2015) for intercomparison between Q-ACSMs or Fig. 1 for comparison of Q-ACSMs to HR-AMS and ToF-ACSM). Average organic matter concentrations during the whole period with $6.9 \mu\text{g m}^{-3}$ (range ≈ 0.7 – $25 \mu\text{g m}^{-3}$) were in the range of typical OA concentrations at this site (Petit et al., 2014), providing good boundary conditions (high signal-to-noise and variability) for PMF source apportionment. For a more detailed analysis of the concentration ranges we refer to Crenn et al. (2015).

3.2 Organic mass spectra

The mass spectrometer discriminates molecular fragments of certain mass-to-charge ratios resulting in the typical stick plot representation of mass spectra. The bulk organic signal is calculated from the sum of the sticks (total integrated signal for a given integer m/z) associated with organic molecules or molecular fragments according to known fragmentation patterns detailed in Allan et al. (2004). This is done under the assumption that with constant boundary conditions the fragmentation is constant as well. The sticks in Fig. 2a represent the median fractions of total organic matter at the respective mass-to-charge ratios for the 13 Q-ACSM instruments during an interruption-free 20 h period (26 November 10:00–27 November 06:00 local time (UTC + 1)). The IQR and the full range are displayed as boxes and whiskers respectively.

There is significant information remaining in the organic molecular fragments. For example fragments at m/z 60 (mainly $\text{C}_2\text{H}_4\text{O}_2^+$) and m/z 73 ($\text{C}_3\text{H}_5\text{O}_2^+$) mostly originate from primary biomass burning particles (Alfarra et al., 2007; Ng et al., 2010; Cubison et al., 2011), there are exceptions in marine environments where the signal at m/z 60 can also be mainly from Na^{37}Cl , see Ovadnevaite et al. (2012). m/z 29 (mainly CHO^+)

as well is often enhanced in wood burning emissions but is also observed from other sources e.g. SOA (Chhabra et al., 2010). The fragments at m/z 43 (mainly $C_2H_3O^+$) and m/z 44 (mainly CO_2^+) can help retrieving information about ageing and oxidation state of secondary organic aerosol (SOA) (Ng et al., 2010, 2011a).

The four fragments mentioned above are shown in Fig. 2b as fraction of the total organic signal for all 15 participating instruments during the 20 h period mentioned above. As already represented in the colour bar of Fig. 2a it is evident that while most fragments have more or less similar contributions to total organic matter (e.g. f29, f43 and f60 in Fig. 2b), there is significant instrument-to-instrument variation of the f44. It is to note that the organic signals at m/z 16, 17 and 18 are also calculated from m/z 44 according to the fragmentation patterns highlighting the importance of the f44 variations (cf Fig. 2a). A comparison of the mass spectra after the stick at m/z 44 and all related peaks were removed shows very similar relative spectra (IQR/median < 20 % for most m/z , cf. Fig. S1 in the Supplement). Only m/z 29 which is mostly CHO^+ still shows a small increase (see Fig. S1b). This may either indicate a connection to m/z 44 (CO_2^+) or a small influence of air interferences.

Figure 2c shows that estimated O : C ratios based on f44 (Aiken et al., 2008) in this study varied from 0.41 to 0.77 for the same ambient aerosol. An elemental analysis of the HR-AMS data, however yielded an O : C ratio of 0.38. This is close to the O : C ratio calculated from the formula of Aiken et al. (2008) for the HR-AMS spectrum (0.42). The consistency of the HR-AMS elemental analysis was confirmed by comparison to a known organic mixture beforehand. As a consequence the “real” O : C value during the intercomparison campaign most likely lies at the low end of Fig. 2c and the ACSMs overestimate O : C.

The fraction of m/z 44 to total organic matter measured (f44) continuously varies compared to the mean between factors of 0.6 and 1.3 (from 8.5 and 18.2 %, Fig. 2b). Although the absolute value of f44 that is measured by different instruments is variable, all the instruments measure similar trends for f44. The ratio of f44 between the instruments with even the highest and lowest f44 values, for example, is generally con-

Intercomparison of ME-2 organic source apportionment

R. Fröhlich et al.

Title Page

Abstract

Introduction

Conclusions

References

Tables

Figures



Back

Close

Full Screen / Esc

Printer-friendly Version

Interactive Discussion



stant over time and does not vary with aerosol composition (see Fig. S2). Moreover, the precision of an individual, stable instrument is good and relative changes observed for any given instrument can be unambiguously interpreted. Thus, source apportionment analyses are not compromised, and indeed are only slightly affected as discussed hereafter.

Measurements of organic standards could be used to calibrate and allow for the intercomparison of the absolute f44 values observed in different ACSM instruments. However, in the absence of these calibrations, caution should be exercised in quantitatively comparing f44 values obtained by different ACSM instruments. This includes application of the f44 vs. f43 “triangle plot” (Ng et al., 2010) that is widely used to describe oxygenated organic aerosol (OOA) factors and comparisons of O : C values derived from ACSM f44 values.

A direct influence of the vaporiser temperature on this variability is ruled out by ACSM measurements of ambient reference aerosols (nebulisation of filter extracts, see Dällenbach et al., 2015, for method description) at different vaporiser temperatures. Relative organic spectra remained constant over a wide range of temperatures (see Fig. S3 and caption) as it was already shown for several organic standards by Canagaratna et al. (2015). Also the fragmentation of inorganic molecules remained constant over a range of at least $550 \pm 70^\circ\text{C}$.

The f44 variability is observed to be larger in the ACSM instruments than the AMS instruments (Ng et al., 2011c; Canagaratna et al., 2007). The ACSM and AMS instruments are based on the same particle vaporisation and ionisation schemes (using the identical particle vaporiser), but they are operated with different open/closed or open/filter switching cycles required for background subtraction. AMS instruments are typically operated with a faster switching cycle ($< 5\text{ s}$) than the Q-ACSMs ($\sim 30\text{ s}$), which in turn have shorter open times than the ToF-ACSM with the “fast-mode MS” (Kimmel et al., 2011) setting employed in this campaign (480 s open/120 s closed). It is noted that a fast filter switching scheme analogous to that of the Q-ACSM has now been implemented for the ToF-ACSM. The different switching times may result in

Intercomparison of ME-2 organic source apportionment

R. Fröhlich et al.

Title Page

Abstract

Introduction

Conclusions

References

Tables

Figures



Back

Close

Full Screen / Esc

Printer-friendly Version

Interactive Discussion



time in the diurnal variation (Fig. 4) are characteristic of clearly resolved COA factors in previous studies and support the present interpretation.

The secondary factor #3 consists of highly oxidised (high f44) organic aerosol (OOA). The diurnal cycle is more or less flat and the overall concentrations are more driven by meteorology than by emissions (see OOA time trace in Fig. 3a). This is supported by the stronger correlation of OOA to sulphate ($R^2 = 0.43$), ammonium ($R^2 = 0.54$), and nitrate ($R^2 = 0.47$, see Fig. S4d) than for the other three factors (cf. Table S4). As is frequently the case for winter campaigns, the OOA could not be further separated into oxygenation/volatility-dependent fractions (Lanz et al., 2010; Zhang et al., 2011).

The most descriptive features in the mass spectrum of factor #4 identifying it as BBOA are the oxygenated peaks at m/z 60 ($C_2H_4O_2^+$) and m/z 73 ($C_3H_5O_2^+$). They are associated with fragmentation of levoglucosan which is produced in the devolatilisation of cellulose making it a good tracer for biomass burning emissions (Simoneit et al., 1999; Q. H. Hu et al., 2013). Generally BBOA profiles from different measurement sites are less uniform than e.g. HOA profiles because of the higher variability of fuel and burning conditions (Weimer et al., 2008; Grieshop et al., 2009; Heringa et al., 2011, 2012; Crippa et al., 2014). The BBOA factor profiles from this study contain relatively high f44 which may be an indication of ageing and oxidation prior to detection. Similar BBOA spectra were observed before, e.g. in winter in Paris (Crippa et al., 2013a) and in Zurich (Canonaco et al., 2013). The diurnal variation shows a steep increase in the afternoon and evening and a subsequent decrease after midnight, corresponding with domestic heating habits. In Fig. S4c the BBOA factor shows very good correlation with BC_{wb} from the aethalometer ($R^2 = 0.90$) and good correlation to gas-phase methanol ($R^2 = 0.76$) and acetonitrile ($R^2 = 0.48$) measured with a PTR-MS. In winter wood combustion is a significant source for primary and secondary methanol (Holzinger et al., 1999; Jacob et al., 2005; Gaeggeler et al., 2008; Akagi et al., 2013).

Overall factor contributions in the analysis of the HR-ToF-AMS data are: HOA 12.7 %, COA 16.0 %, OOA 38.2 %, BBOA 33.1 %. Relative contributions, number and type of

Intercomparison of ME-2 organic source apportionment

R. Fröhlich et al.

Title Page

Abstract

Introduction

Conclusions

References

Tables

Figures



Back

Close

Full Screen / Esc

Printer-friendly Version

Interactive Discussion



Intercomparison of ME-2 organic source apportionment

R. Fröhlich et al.

Title Page

Abstract

Introduction

Conclusions

References

Tables

Figures



Back

Close

Full Screen / Esc

Printer-friendly Version

Interactive Discussion



ways possible and a more common approach is the adaptation of reference spectra from a database of previous experiments. Therefore the ME-2 results acquired with the use of the database profiles HOA_{Paris} and COA_{Paris} are shown as well for comparison. The influence of an alternative anchor (see Fig. 7, top panel, and Sect. 3.5.3) proved to be only marginal. The source apportionment of the ToF-ACSM data produces clearer diurnal trends due to less scatter in the time series and higher temporal resolution compared to the Q-ACSM data. This facilitates source identification. In this study, however, for a clear separation of all four factors without the extra information of HR fitted spectra, the additional controls (e.g. possibility to introduce anchor spectra) of the ME-2 package were necessary for the source apportionment of both, ToF-ACSM and Q-ACSM data.

Optimal a values in each case were determined by systematic variation of the a value in relation to increases or decreases of the correlation coefficient R^2 of the factor time series with external tracers. The correlations which were maximised for the determination of the best a values were: BBOA factor with BC_{wb}, OOA factor with inorganic SO₄ and HOA factor with BC_{ff} and NO_x. Correlation maxima (R^2) are listed in Table 2. Changes in a value usually affected mainly the correlations of the HOA factor while the correlations of the BBOA and OOA factors were quite stable. On that account two correlations to HOA were made. The sum of the two HOA R^2 is maximised. For COA no reliable external tracer was measured. For all factors good correlations with the respective external measurement were reached: BBOA – BC_{wb}: median $R^2 = 0.87$ (range 0.85–0.94), HOA – BC_{ff}: median $R^2 = 0.65$ (range 0.52–0.73), HOA – NO_x: median $R^2 = 0.62$ (range 0.52–0.77), OOA – SO₄: median 0.72 (range 0.51–0.79).

The applied strategy was: increase of a in steps of $\Delta a = 0.05$ until a maximum R^2 (coefficient of correlation between time series of resulting factors and corresponding external tracers) is found. If more than one factor profile is constrained, first both a values are varied simultaneously until a maximum R^2 is found. From this point, the a value of each reference profile is varied separately in both direction while the other

stays constant. This way a large range of a values could be explored for each instrument.

It is to note that of course also the BC source apportionment and other external data used for this sensitivity analysis are prone to uncertainties. The approach detailed above therefore should, if applied elsewhere, always be used with caution. In the presented case the optimisation of a values also assured the comparability of the 15 solutions used for the intercomparison of the ME-2 method. A thorough discussion of the uncertainties of the BC source apportionment method and a comparison to other source apportionment methods can be found in Favez et al. (2010).

Optimised a values for each instrument are shown in Table 1. In some cases no clear maximum of the temporal correlation to external tracers but a plateau of the correlation coefficient R^2 could be found and the largest possible a value is noted in Table 1. This indicates a stable HOA factor. The COA factor which could not be resolved in the pure PMF of the ACSM data sets is less stable and therefore generally needs a tighter constraint, i.e. a lower a value (see right column of Table 1). This is necessary to avoid as much as possible potential mixing of COA and BBOA factors. Similar diurnal cycles of heating and cooking activities (both sources have the highest emissions during the evening hours) pose a risk for factor mixing especially in the Q-ACSM data sets which have lower mass resolution and generally less precision. Two weeks of Q-ACSM measurement result in about 700 mass spectra of which only ~ 30 are including lunchtime COA emissions and the emission peak of COA aerosol in the evening overlaps with wood burning emissions. In addition COA emissions may be significantly lower and partly transported in contrast to measurements at an urban site. All this may put COA at the edge of ME-2 resolvability. Due to this the Q-ACSM COA factor may still contain some mixed-in BBOA fraction or the other way round. Also the fact that the contribution of the COA factor stays well above zero during the night can be an indicator of some remaining factor mixing which cannot be resolved by ME-2 for this data set, of additional sources emitting COA-like aerosol more permanently like food industry or of regional transport or of the lower mixing height of the planetary boundary layer during night. Due

Intercomparison of ME-2 organic source apportionment

R. Fröhlich et al.

[Title Page](#)[Abstract](#)[Introduction](#)[Conclusions](#)[References](#)[Tables](#)[Figures](#)[Back](#)[Close](#)[Full Screen / Esc](#)[Printer-friendly Version](#)[Interactive Discussion](#)

to the first two points, real COA emissions may be somewhat lower than indicated by the COA factor and the factor is named COA-like in the following. For HOA_{indv} a smaller range of a values ($a = 0.01-0.10$; $\Delta a = 0.01$) was explored to maintain similarity to the extracted profiles.

3.5 Intercomparison of source apportionment results

3.5.1 Time series

Diurnal variation and factor profiles of all 15 solutions (13 × Q-ACSM, 1 × ToF-ACSM, 1 × HR-ToF-AMS) are displayed in Fig. 5 (for full time series see Fig. S7) and Figs. S13 and S14. To avoid influence of a potentially varying CE, the diurnal plots show the relative fractions of the total apportioned organic matter for the respective source factors instead of absolute concentrations. The diurnal variation plots of the four factors show the median of all Q-ACSMs (black) and the IQR as well as the 10–90 percentile range together with the diurnal variation of AMS (pink) and ToF-ACSM (green) factors. To facilitate comparison and to avoid a too large influence of the drift observed in the ToF-ACSM (see Sect. 2.5), all diurnal time traces (Q-ACSMs, HR-ToF-AMS and ToF-ACSM) were calculated only for the measurement period between 20 November and 2 December, discarding the first four days of measurement in which the observed exponentially decaying drift had the largest influence. Morning and evening rush hour peaks in the HOA as well as lunch and dinner time peaks in the COA-like factor are easily discernible around 1 p.m. and 9 p.m. The fraction of BBOA significantly increases in the evening when domestic heating activities are highest and decreases again after midnight with a small plateau in the morning when people are waking up. The apparent decrease of the OOA relative contribution in the evening can be attributed to the increase of BBOA since the absolute concentrations of OOA show no diurnal trends (cf. Fig. S7). The observed trend of the diurnal variations are similar in all 15 instruments. The full time series of all devices normalised to the total concentration measured with the HR-ToF-AMS are shown in Fig. S7. Correlations of these normalised factor time se-

Intercomparison of ME-2 organic source apportionment

R. Fröhlich et al.

Title Page

Abstract

Introduction

Conclusions

References

Tables

Figures



Back

Close

Full Screen / Esc

Printer-friendly Version

Interactive Discussion



Intercomparison of ME-2 organic source apportionment

R. Fröhlich et al.

Title Page

Abstract

Introduction

Conclusions

References

Tables

Figures



Back

Close

Full Screen / Esc

Printer-friendly Version

Interactive Discussion



ries to the median of all instruments are illustrated in the Supplement in Figs. S8–S11. Slopes range between 0.73–1.27 (HOA), 0.62–1.43 (COA-like), 0.77–1.23 (BBOA) and 0.66–1.28 (OOA) with correlation coefficients R^2 between 0.63–0.94 (HOA, median R^2 : 0.91), 0.55–0.91 (COA-like, median R^2 : 0.85), 0.90–0.98 (BBOA, median R^2 : 0.95) and 0.72–0.95 (OOA, median R^2 : 0.91).

Diurnal variation of the relative factor contributions from the HR-AMS and the ToF-ACSM data sets are largely within the range of the Q-ACSMs. The morning peak of the HOA is slightly smaller in the HR-AMS than in the other devices (morning traffic peak contributions: 22.5 % (HR-AMS), 27.7 % (median Q-ACSMs), 30.4 % (ToF-ACSM)) and the source apportionment of the ToF-ACSM data set yielded slightly lower OOA but higher BBOA concentrations (cf. Fig. 7, bottom panel). It is noted that the non-uniform time steps the Q-ACSM data is recorded at, and several unplanned measurement interruptions of some of the instruments made it impossible to completely synchronise all devices. This contributes an unknown, likely small fraction of the total uncertainty.

The lower panel of Fig. 5 shows the diurnal variation of the model residuals scaled to the total organic concentrations. Residuals of ToF-ACSM and Q-ACSMs fluctuate around zero and are always within a range smaller than $\pm 2\%$ of total organic concentrations. In the evening hours when total organic concentrations are highest the scaled residuals tend to be slightly larger. The HR-AMS residuals, however, are higher and purely positive. A more detailed analysis shows that all m/z channels are affected to a similar extent. The reason for the purely positive residuals is unknown, but no significant temporal variation and no significant change or decrease of the residuals even in PMF runs with high number of factors (> 10) indicate that the residuals are not connected with additional factors missing in the current analysis.

3.5.2 Profiles

The median factor profiles of the HOA, COA-like, BBOA and OOA factors of the 13 Q-ACSMs are shown as sticks in Fig. 6. IQR of each individual stick is displayed as a box while the full range is shown with the whiskers. Colours denote the width of the IQR

box relative to the median. For the BBOA and OOA factors the m/z range between 50 and 100 is enlarged in separate insets. The typical features of each factor are similar to the HR data in Sect. 3.3.

The aliphatic hydrocarbon signals characteristic for HOA have relatively stable contributions to the HOA source spectrum (box $\lesssim 15\%$, green colour) in all instruments. The variation of m/z 43 is slightly higher ($\approx 25\%$, yellow) and the mass-to-charge ratios 29 and 44 (and 16–18 which are calculated directly from m/z 44, see Allan et al., 2004) have quite large boxes ($> 50\%$, violet). These fragments are also partly apportioned to BBOA and OOA which could indicate a minor mixing of these sources into the HOA factor for some instruments. Considering the full range (whiskers) instrument #13 (see Fig. S13) represents an outlier with high m/z 44 in the HOA. It is noted that in most ME-2 source apportionments this solution would have been discarded and an approach with a constrained externally measured HOA profile would have been favoured (similar to the approach used to calculate the second bars from the left in Fig. 7, top panel). For the sake of comparability the solution with the individually extracted HOA profile of instrument #13 is still included in this analysis. Other contributing m/z channels which exhibit a larger variability of more than 30% in the HOA profiles are 26, 27, 53, 66, 77 and 91.

The second panel of Fig. 6 shows the variation of the COA source profiles which were constrained with low a values. It is noted that the method of adding constraints to the ME-2 output naturally has an effect on its maximum possible variability. Therefore no variations $\gtrsim 20\%$ are observed.

The BBOA profile is shown in the third panel. The variations of the important markers at m/z 29, 60 and 73 show the smallest variations ($\lesssim 25\%$). The f44 however exhibits a variability of $\approx 50\%$. A more detailed look at the BBOA profiles in Fig. S14 shows a dependency on total f44. While instruments with lower total f44 mostly have a lower f44 in the BBOA spectrum, devices with higher f44 on the other hand also tend to have higher f44 in their BBOA spectrum. This should be kept in mind for the application of

Intercomparison of ME-2 organic source apportionment

R. Fröhlich et al.

Title Page

Abstract

Introduction

Conclusions

References

Tables

Figures



Back

Close

Full Screen / Esc

Printer-friendly Version

Interactive Discussion



f44 to characterise ageing of biomass burning plumes (as it could be shown for AMS data by Cubison et al., 2011) from ACSM datasets.

The OOA factor profile shows only slightly smaller absolute variation (size of box) of f44 as the BBOA profile, but since here f44 is larger in general, the resulting size of the box in relation to the median is only on the order of $\approx 20\%$. Considering the full range f44 varies by about 40%, similar to the variation of f44 in the input organic mass spectra. Again, a look at Fig. S14 reveals an increasing f44 in the OOA source profile with increasing total f44. There are only few additional m/z channels having significant contributions to OOA. The magnification of the region above m/z 50 shows only very low signals with high variations which predominantly can be considered noise.

The fact that the f44 has a high instrument-to-instrument variability in all unconstrained factors has important implications for the application of reference profiles measured with an AMS or another ACSM to ACSM data sets. Constraints on m/z 44 should be avoided or loosened as much as possible. Alternatively the f44 in such reference profiles should be subjected to a sensitivity test (e.g. by manually changing the f44 of a reference profile).

The source profiles of the ME-2 analysis of the ToF-ACSM data set are shown in Fig. S12 together with box and whisker plots of the Q-ACSM profiles. Generally the ToF-ACSM source profiles lie well within the range of the Q-ACSMs. Since the ToF-ACSM had the highest f44 of all instruments all factor profiles lie at the upper end of the Q-ACSM f44 range. The signals at higher mass-to-charge ratios are a bit smaller. This could either be due to an overestimation of the relative ion transmission (RIT) correction performed on the Q-ACSM mass spectral data (see RIT discussion in the Supplement) or to loss of smaller signals in the ToF-ACSM caused by the operational issue with the detector amplification detailed in Sect. 2.5. The latter is unlikely but cannot be completely excluded.

Intercomparison of ME-2 organic source apportionment

R. Fröhlich et al.

Title Page

Abstract

Introduction

Conclusions

References

Tables

Figures



Back

Close

Full Screen / Esc

Printer-friendly Version

Interactive Discussion



measured (largest deviations at #1–#3 and #5 and #6), leading to the assumption that the choice of reference HOA spectrum is not too crucial if the *a* values are optimised.

Median and average contributions of each of the four factors are summarised in Table 3 together with the corresponding SDs. HOA contributed $14.3 \pm 2.2\%$, COA $15.0 \pm 3.4\%$, OOA $41.5 \pm 5.7\%$ and BBOA $29.3 \pm 5.0\%$ to the total organic mass. It is noted that average concentrations over the 15 day period were $6.9 \mu\text{g m}^{-3}$ (range $\approx 0.7\text{--}25 \mu\text{g m}^{-3}$, cf. Fig. 1) and higher or lower signal-to-noise ratios or differences in the source time series variability have an effect on the accuracy of the results. Usually lower average concentrations or less temporal variability will increase the uncertainties while higher average concentrations or increased temporal variability will decrease the uncertainties. The uncertainties found in this study are shown more in detail in Fig. 7 (bottom panel). There the individual deviations of all factors from the median are shown in percent for all participating instruments. The $\pm 15\%$ region is indicated by the dashed line and the $\pm 30\%$ region by the solid line. Most deviations lie within the $\pm 15\%$ region, especially HOA, OOA and BBOA have only few outliers (HOA: 3, BBOA: 4, OOA: 3) while COA-like factor has significantly more (7 outliers). This emphasises the already discussed notion that COA was the most difficult factor to quantify because of the temporally low occurrence (lunchtime) of significant events and its partial concurrence with the BBOA in the evening hours. Therefore COA also possesses the highest uncertainties in this study.

Over- and underestimation of all four factors looks more or less randomly distributed, no significant dependence on f44 is noticeable. This suggests that the differences in the input data matrix (cf. Sect. 3.2), mainly the f44, do not contribute significantly to the already relatively small discrepancies of the factor contributions between the 15 instruments (Table 3) even though source spectra can differ significantly between instruments (cf. Sect. 3.5.2). This indicates a correct allocation of the additional *m/z* 44 signal which may originate from pyrolysed organic compounds to the original aerosol source.

Intercomparison of ME-2 organic source apportionment

R. Fröhlich et al.

Title Page

Abstract

Introduction

Conclusions

References

Tables

Figures



Back

Close

Full Screen / Esc

Printer-friendly Version

Interactive Discussion



Figure S15 shows the same results in terms of z score values (calculated in accordance with ISO13528, 2005), a dimensionless statistical quantity (see Eq. S1) evaluating the performance of each source apportionment solution with respect to the others (Karagulian and Belis, 2012). The same method was employed in part I of this study by Crenn et al. (2015). With two exceptions (HOA in instrument #13 and OOA in the ToF-ACSM) all results lie in the “ok” and “acceptable” regime defined by $|z| \leq 2$.

It is noted that the stated uncertainties are only the relative uncertainties of the source apportionment, not taking into account the additional variation of total measured organic mass between instruments, which is assessed in part 1 of this study (Crenn et al., 2015). Average concentration and first SD in $\mu\text{g m}^{-3}$ of each source are given in Table S6, representing the combination of both sources of uncertainty.

3.5.4 ACSM specific recommendations

Crippa et al. (2014) developed a standardised approach for ME-2 analyses of AMS measurements in addition to the recommendations given by Ulbrich et al. (2009). Since ACSM data is basically identical to UMR AMS data with reduced temporal resolution, a similar approach is recommended for ACSM data sets. Additionally, several ACSM specific points are suggested by the current study:

- Profile constraints on the m/z 44 signal should be avoided or kept as loose as possible (high a value for m/z 44).
- If constraints are applied to the m/z 44 signal, a sensitivity analysis by manual modification of the relative amount of the m/z 44 signal is recommended.
- Anchor profiles constructed from the studied dataset are preferable to database profiles. These profiles can often be extracted from solutions with additional factors (e.g. this study) or from separate PMF on parts of the dataset with high fractional contributions of a factor (e.g. period with nearby forest fires or high primary traffic emissions).

Intercomparison of ME-2 organic source apportionment

R. Fröhlich et al.

Title Page

Abstract

Introduction

Conclusions

References

Tables

Figures



Back

Close

Full Screen / Esc

Printer-friendly Version

Interactive Discussion



The fraction of organic mass occurring at m/z 44 (f44) varied between factors of 0.6 and 1.3 compared to the mean across all instruments. Such differences should be considered in comparing estimated O:C ratios and retrieved factor profiles between ACSMs. The f44 discrepancies do have significant influence on resulting factor profiles of ME-2/PMF analyses but no significant influence on total factor contributions was noticed.

A good agreement of relative factor contributions over all 15 instruments was found. On average HOA contributed $14.3 \pm 2.2\%$, COA $15.0 \pm 3.4\%$, OOA $41.5 \pm 5.7\%$ and BBOA $29.3 \pm 5.0\%$. The listed first SDs give a measure for the uncertainty of the ME-2 source apportionment related to the measurement technique. From these numbers a relative deviation from the mean combined over all factors of $\pm 17.2\%$ was calculated.

The Supplement related to this article is available online at doi:10.5194/amtd-8-1559-2015-supplement.

Acknowledgements. This work was conducted in the frame of the ACTRIS program (European Union Seventh Framework Program (FP7/2007-2013), grant agreement no 262254). The authors acknowledge the French Agency of Environment and Energy Management (ADEME grants 1262C0022 and 1262C0039), the CaPPA (Chemical and Physical Properties of the Atmosphere) project (ANR-10-LABX-005) funded by the French National Research Agency (ANR) through the PIA (Programme d'Investissement d'Avenir), the EU-FEDER CORSiCA, Eurostars E!4825 and KROP, financed by the Slovenian Ministry of Economic Development and Technology, and ChArMEx projects. J. G. Slowik acknowledges support from the Swiss National Science Foundation (SNSF) through the Ambizione program (PZ00P2_131673). V. Crenn acknowledges the DIM R2DS program for his post-doctoral grant. J. Ovadnevaite and C. D. O'Dowd acknowledge HEA-PRTLI4 and NUIG's Research Support Fund. CIEMAT contribution has been partially funded by CGL2011-16124-E, CGL2011-27020 actions from the Spanish National R&D Programme, and AEROCLIMA (Fundacion Ramon Areces, CIVP16A1811). IDAEA CSIC was partially funded by the Spanish Ministry of Economy and Competitiveness and FEDER funds under the PRISMA (CGL2012-39623-C02-1) project.

References

- Aiken, A. C., DeCarlo, P. F., Kroll, J. H., Worsnop, D. R., Huffman, J. A., Docherty, K. S., Ulbrich, I. M., Mohr, C., Kimmel, J. R., Sueper, D., Sun, Y., Zhang, Q., Trimborn, A., Northway, M., Ziemann, P. J., Canagaratna, M. R., Onasch, T. B., Alfarra, M. R., Prevot, A. S. H., Dommen, J., Duplissy, J., Metzger, A., Baltensperger, U., and Jimenez, J. L.: O/C and OM/OC ratios of primary, secondary, and ambient organic aerosols with high-resolution time-of-flight aerosol mass spectrometry, *Environ. Sci. Technol.*, 42, 4478–4485, doi:doi:10.1021/es703009q, 2008. 1565, 1567, 1573, 1608
- Aiken, A. C., Salcedo, D., Cubison, M. J., Huffman, J. A., DeCarlo, P. F., Ulbrich, I. M., Docherty, K. S., Sueper, D., Kimmel, J. R., Worsnop, D. R., Trimborn, A., Northway, M., Stone, E. A., Schauer, J. J., Volkamer, R. M., Fortner, E., de Foy, B., Wang, J., Laskin, A., Shutthanandan, V., Zheng, J., Zhang, R., Gaffney, J., Marley, N. A., Paredes-Miranda, G., Arnott, W. P., Molina, L. T., Sosa, G., and Jimenez, J. L.: Mexico City aerosol analysis during MILAGRO using high resolution aerosol mass spectrometry at the urban supersite (T0) – Part 1: Fine particle composition and organic source apportionment, *Atmos. Chem. Phys.*, 9, 6633–6653, doi:10.5194/acp-9-6633-2009, 2009. 1563, 1575
- Aiken, A. C., de Foy, B., Wiedinmyer, C., DeCarlo, P. F., Ulbrich, I. M., Wehrli, M. N., Szidat, S., Prevot, A. S. H., Noda, J., Wacker, L., Volkamer, R., Fortner, E., Wang, J., Laskin, A., Shutthanandan, V., Zheng, J., Zhang, R., Paredes-Miranda, G., Arnott, W. P., Molina, L. T., Sosa, G., Querol, X., and Jimenez, J. L.: Mexico city aerosol analysis during MILAGRO using high resolution aerosol mass spectrometry at the urban supersite (T0) – Part 2: Analysis of the biomass burning contribution and the non-fossil carbon fraction, *Atmos. Chem. Phys.*, 10, 5315–5341, doi:10.5194/acp-10-5315-2010, 2010. 1563
- Akagi, S. K., Yokelson, R. J., Burling, I. R., Meinardi, S., Simpson, I., Blake, D. R., McMeeking, G. R., Sullivan, A., Lee, T., Kreidenweis, S., Urbanski, S., Reardon, J., Griffith, D. W. T., Johnson, T. J., and Weise, D. R.: Measurements of reactive trace gases and variable O₃ formation rates in some South Carolina biomass burning plumes, *Atmos. Chem. Phys.*, 13, 1141–1165, doi:10.5194/acp-13-1141-2013, 2013. 1577
- Alfarra, M. R., Prevot, A. S. H., Szidat, S., Sandradewi, J., Weimer, S., Lanz, V. A., Schreiber, D., Mohr, M., and Baltensperger, U.: Identification of the mass spectral signature of organic aerosols from wood burning emissions, *Environ. Sci. Technol.*, 41, 5770–5777, doi:10.1021/es062289b 2007. 1563, 1572

AMTD

8, 1559–1613, 2015

Intercomparison of ME-2 organic source apportionment

R. Fröhlich et al.

Title Page

Abstract

Introduction

Conclusions

References

Tables

Figures



Back

Close

Full Screen / Esc

Printer-friendly Version

Interactive Discussion



**Intercomparison of
ME-2 organic source
apportionment**

R. Fröhlich et al.

Title Page

Abstract

Introduction

Conclusions

References

Tables

Figures

◀

▶

◀

▶

Back

Close

Full Screen / Esc

Printer-friendly Version

Interactive Discussion



- Allan, J. D., Delia, A. E., Coe, H., Bower, K. N., Alfarra, M., Jimenez, J. L., Middlebrook, A. M., Drewnick, F., Onasch, T. B., Canagaratna, M. R., Jayne, J. T., and Worsnop, D. R.: A generalised method for the extraction of chemically resolved mass spectra from Aerodyne aerosol mass spectrometer data, *J. Aerosol Sci.*, 35, 909–922, 2004. 1565, 1571, 1572, 1583
- 5 Allan, J. D., Williams, P. I., Morgan, W. T., Martin, C. L., Flynn, M. J., Lee, J., Nemitz, E., Phillips, G. J., Gallagher, M. W., and Coe, H.: Contributions from transport, solid fuel burning and cooking to primary organic aerosols in two UK cities, *Atmos. Chem. Phys.*, 10, 647–668, doi:10.5194/acp-10-647-2010, 2010. 1563, 1576
- Bond, T. C. and Bergstrom, R. W.: Light absorption by carbonaceous particles: an investigative review, *Aerosol Sci. Tech.*, 40, 27–67, doi:10.1080/02786820500421521, 2006. 1568
- 10 Boucher, O., D., R., Artaxo, P., Bretherton, C., Feingold, G., Forster, P., Kerminen, V.-M., Kondo, Y., Liao, H., Lohmann, U., Rasch, P., Satheesh, S. K., Sherwood, S., Stevens, B., and Zhang, X. Y.: Clouds and aerosols, in: *Climate Change 2013: The Physical Science Basis. Contribution of Working Group I to the Fifth Assessment Report of the Intergovernmental Panel on Climate Change*, edited by: Stocker, T., Qin, D., Plattner, G.-K., Tignor, M., Allen, S., Boschung, J., Nauels, A., Xia, Y., V., B., and Midgley, P. M., Cambridge University Press, Cambridge, UK, New York, NY, USA, 571–657, 2013. 1562
- 15 Bressi, M., Sciare, J., Ghersi, V., Mihalopoulos, N., Petit, J.-E., Nicolas, J. B., Moukhtar, S., Rosso, A., Féron, A., Bonnaire, N., Poulakis, E., and Theodosi, C.: Sources and geographical origins of fine aerosols in Paris (France), *Atmos. Chem. Phys.*, 14, 8813–8839, doi:10.5194/acp-14-8813-2014, 2014. 1564
- 20 Brown, S. G., Lee, T., Norris, G. A., Roberts, P. T., Collett Jr., J. L., Paatero, P., and Worsnop, D. R.: Receptor modeling of near-roadway aerosol mass spectrometer data in Las Vegas, Nevada, with EPA PMF, *Atmos. Chem. Phys.*, 12, 309–325, doi:10.5194/acp-12-309-2012, 2012. 1569
- 25 Canagaratna, M., Jayne, J., Jimenez, J., Allan, J., Alfarra, M., Zhang, Q., Onasch, T., Drewnick, F., Coe, H., Middlebrook, A., Delia, A., Williams, L., Trimborn, A., Northway, M., DeCarlo, P., Kolb, C., Davidovits, P., and Worsnop, D.: Chemical and microphysical characterization of ambient aerosols with the aerodyne aerosol mass spectrometer, *Mass Spectrom. Rev.*, 26, 185–222, 2007. 1566, 1574
- 30 Canagaratna, M. R., Jimenez, J. L., Kroll, J. H., Chen, Q., Kessler, S. H., Massoli, P., Hildebrandt Ruiz, L., Fortner, E., Williams, L. R., Wilson, K. R., Surratt, J. D., Donahue, N. M., Jayne, J. T., and Worsnop, D. R.: Elemental ratio measurements of organic compounds using

**Intercomparison of
ME-2 organic source
apportionment**

R. Fröhlich et al.

Title Page

Abstract

Introduction

Conclusions

References

Tables

Figures



Back

Close

Full Screen / Esc

Printer-friendly Version

Interactive Discussion



aerosol mass spectrometry: characterization, improved calibration, and implications, *Atmos. Chem. Phys.*, 15, 253–272, doi:10.5194/acp-15-253-2015, 2015. 1574

Canonaco, F., Crippa, M., Slowik, J. G., Baltensperger, U., and Prévôt, A. S. H.: SoFi, an IGOR-based interface for the efficient use of the generalized multilinear engine (ME-2) for the source apportionment: ME-2 application to aerosol mass spectrometer data, *Atmos. Meas. Tech.*, 6, 3649–3661, doi:10.5194/amt-6-3649-2013, 2013. 1563, 1569, 1570, 1576, 1577

Carslaw, K. S., Boucher, O., Spracklen, D. V., Mann, G. W., Rae, J. G. L., Woodward, S., and Kulmala, M.: A review of natural aerosol interactions and feedbacks within the Earth system, *Atmos. Chem. Phys.*, 10, 1701–1737, doi:10.5194/acp-10-1701-2010, 2010. 1562

Carslaw, K. S., Lee, L. A., Reddington, C. L., Pringle, K. J., Rap, A., Forster, P. M., Mann, G. W., Spracklen, D. V., Woodhouse, M. T., Regayre, L. A., and Pierce, J. R.: Large contribution of natural aerosols to uncertainty in indirect forcing, *Nature*, 503, 67–71, 2013. 1562

Chhabra, P. S., Flagan, R. C., and Seinfeld, J. H.: Elemental analysis of chamber organic aerosol using an aerodyne high-resolution aerosol mass spectrometer, *Atmos. Chem. Phys.*, 10, 4111–4131, doi:10.5194/acp-10-4111-2010, 2010. 1573

Cohen, A. J., Ross Anderson, H., Ostro, B., Pandey, K. D., Krzyzanowski, M., Kunzli, N., Gutschmidt, K., Pope, A., Romieu, I., Samet, J. M., and Smith, K.: The global burden of disease due to outdoor air pollution, *J. Toxicol. Env. Heal. A*, 68, 1301–1307, 2005. 1562

Collaud Coen, M., Weingartner, E., Apituley, A., Ceburnis, D., Fierz-Schmidhauser, R., Flentje, H., Henzing, J. S., Jennings, S. G., Moerman, M., Petzold, A., Schmid, O., and Baltensperger, U.: Minimizing light absorption measurement artifacts of the Aethalometer: evaluation of five correction algorithms, *Atmos. Meas. Tech.*, 3, 457–474, doi:10.5194/amt-3-457-2010, 2010. 1567

Crenn, V., Sciare, J., Croteau, P. L., Favez, O., Verlhac, S., Belis, C. A., Fröhlich, R., Aas, W., Äijälä, M., Alastuey, A., Artiñano, B., Baisnée, D., Baltensperger, U., Bonnaire, N., Bressi, M., Canagaratna, M., Canonaco, F., Carbone, C., Cavalli, F., Coz, E., Cubison, M. J., Gietl, J. K., Green, D. C., Heikkinen, L., Lunder, C., Minguillón, M. C., Močnik, G., O'Dowd, C. D., Ovadnevaite, J., Petit, J.-E., Petralia, E., Poulain, L., Prévôt, A. S. H., Priestman, M., Riffault, V., Ripoll, A., Sarda-Estève, R., Slowik, J., Setyan, A., and Jayne, J. T.: ACTRIS ACSM intercomparison: Part 1 – Intercomparison of concentration and fragment results from 13 individual co-located aerosol chemical speciation monitors (ACSM), *Atmos. Meas. Tech. Discuss.*, submitted, 2015. 1563, 1564, 1565, 1566, 1570, 1571, 1572, 1587

Intercomparison of ME-2 organic source apportionment

R. Fröhlich et al.

[Title Page](#)[Abstract](#)[Introduction](#)[Conclusions](#)[References](#)[Tables](#)[Figures](#)[Back](#)[Close](#)[Full Screen / Esc](#)[Printer-friendly Version](#)[Interactive Discussion](#)

Crippa, M., DeCarlo, P. F., Slowik, J. G., Mohr, C., Heringa, M. F., Chirico, R., Poulain, L., Freutel, F., Sciare, J., Cozic, J., Di Marco, C. F., Elsassner, M., Nicolas, J. B., Marchand, N., Abidi, E., Wiedensohler, A., Drewnick, F., Schneider, J., Borrmann, S., Nemitz, E., Zimmermann, R., Jaffrezo, J.-L., Prévôt, A. S. H., and Baltensperger, U.: Wintertime aerosol chemical composition and source apportionment of the organic fraction in the metropolitan area of Paris, *Atmos. Chem. Phys.*, 13, 961–981, doi:10.5194/acp-13-961-2013, 2013a. 1563, 1564, 1576, 1577, 1578, 1588

Crippa, M., El Haddad, I., Slowik, J. G., DeCarlo, P. F., Mohr, C., Heringa, M. F., Chirico, R., Marchand, N., Sciare, J., Baltensperger, U., and Prévôt, A. S. H.: Identification of marine and continental aerosol sources in Paris using high resolution aerosol mass spectrometry, *J. Geophys. Res.-Atmos.*, 118, 1950–1963, 2013b. 1563, 1576

Crippa, M., Canonaco, F., Lanz, V. A., Äijälä, M., Allan, J. D., Carbone, S., Capes, G., Ceburnis, D., Dall'Osto, M., Day, D. A., DeCarlo, P. F., Ehn, M., Eriksson, A., Freney, E., Hildebrandt Ruiz, L., Hillamo, R., Jimenez, J. L., Junninen, H., Kiendler-Scharr, A., Kortelainen, A.-M., Kulmala, M., Laaksonen, A., Mensah, A. A., Mohr, C., Nemitz, E., O'Dowd, C., Ovadnevaite, J., Pandis, S. N., Petäjä, T., Poulain, L., Saarikoski, S., Sellegri, K., Swietlicki, E., Tiitta, P., Worsnop, D. R., Baltensperger, U., and Prévôt, A. S. H.: Organic aerosol components derived from 25 AMS data sets across Europe using a consistent ME-2 based source apportionment approach, *Atmos. Chem. Phys.*, 14, 6159–6176, doi:10.5194/acp-14-6159-2014, 2014. 1562, 1563, 1576, 1577, 1587

Cubison, M. J., Ortega, A. M., Hayes, P. L., Farmer, D. K., Day, D., Lechner, M. J., Brune, W. H., Apel, E., Diskin, G. S., Fisher, J. A., Fuelberg, H. E., Hecobian, A., Knapp, D. J., Mikoviny, T., Riemer, D., Sachse, G. W., Sessions, W., Weber, R. J., Weinheimer, A. J., Wisthaler, A., and Jimenez, J. L.: Effects of aging on organic aerosol from open biomass burning smoke in aircraft and laboratory studies, *Atmos. Chem. Phys.*, 11, 12049–12064, doi:10.5194/acp-11-12049-2011, 2011. 1572, 1584

Dällenbach, K. R., Bozzetti, C., K epelová, A., Canonaco, F., Wolf, R., Huang, R.-J., Zotter, P., Crippa, M., Slowik, J. G., Zhang, Y., Szidat, S., Baltensperger, U., Prévôt, A. S. H., and El Haddad, I.: Characterization and source apportionment of organic aerosol using offline aerosol mass spectrometry, *Atmos. Meas. Tech. Discuss.*, in preparation, 2015. 1574

DeCarlo, P. F., Kimmel, J. R., Trimborn, A., Northway, M. J., Jayne, J. T., Aiken, A. C., Gonin, M., Fuhrer, K., Horvath, T., Docherty, K. S., Worsnop, D. R., and Jimenez, J. L.:

**Intercomparison of
ME-2 organic source
apportionment**

R. Fröhlich et al.

[Title Page](#)[Abstract](#)[Introduction](#)[Conclusions](#)[References](#)[Tables](#)[Figures](#)[Back](#)[Close](#)[Full Screen / Esc](#)[Printer-friendly Version](#)[Interactive Discussion](#)

Field-deployable, high-resolution, time-of-flight aerosol mass spectrometer, *Anal. Chem.*, 78, 8281–8289, 2006. 1562

Docherty, K. S., Aiken, A. C., Huffman, J. A., Ulbrich, I. M., DeCarlo, P. F., Sueper, D., Worsnop, D. R., Snyder, D. C., Peltier, R. E., Weber, R. J., Grover, B. D., Eatough, D. J., Williams, B. J., Goldstein, A. H., Ziemann, P. J., and Jimenez, J. L.: The 2005 Study of Organic Aerosols at Riverside (SOAR-1): instrumental intercomparisons and fine particle composition, *Atmos. Chem. Phys.*, 11, 12387–12420, doi:10.5194/acp-11-12387-2011, 2011. 1575

Drewnick, F., Hings, S. S., DeCarlo, P., Jayne, J. T., Gonin, M., Fuhrer, K., Weimer, S., Jimenez, J. L., Demerjian, K. L., Borrmann, S., and Worsnop, D. R.: A new time-of-flight aerosol mass spectrometer (TOF-AMS) – instrument description and first field deployment, *Aerosol Sci. Tech.*, 39, 637–658, 2005. 1562

Drinovec, L., Močnik, G., Zotter, P., Prévôt, A. S. H., Ruckstuhl, C., Coz, E., Rupakheti, M., Sciare, J., Müller, T., Wiedensohler, A., and Hansen, A. D. A.: The “dual-spot” Aethalometer: an improved measurement of aerosol black carbon with real-time loading compensation, *Atmos. Meas. Tech. Discuss.*, 7, 10179–10220, doi:10.5194/amtd-7-10179-2014, 2014. 1567

Faber, P., Drewnick, F., Veres, P. R., Williams, J., and Borrmann, S.: Anthropogenic sources of aerosol particles in a football stadium: real-time characterization of emissions from cigarette smoking, cooking, hand flares, and color smoke bombs by high-resolution aerosol mass spectrometry, *Atmos. Environ.*, 77, 1043–1051, 2013. 1563

Favez, O., El Haddad, I., Piot, C., Boréave, A., Abidi, E., Marchand, N., Jaffrezo, J.-L., Besombes, J.-L., Personnaz, M.-B., Sciare, J., Wortham, H., George, C., and D’Anna, B.: Intercomparison of source apportionment models for the estimation of wood burning aerosols during wintertime in an Alpine city (Grenoble, France), *Atmos. Chem. Phys.*, 10, 5295–5314, doi:10.5194/acp-10-5295-2010, 2010. 1580

Fröhlich, R., Cubison, M. J., Slowik, J. G., Bukowiecki, N., Prévôt, A. S. H., Baltensperger, U., Schneider, J., Kimmel, J. R., Gonin, M., Rohner, U., Worsnop, D. R., and Jayne, J. T.: The ToF-ACSM: a portable aerosol chemical speciation monitor with TOFMS detection, *Atmos. Meas. Tech.*, 6, 3225–3241, doi:10.5194/amt-6-3225-2013, 2013. 1562, 1578

Gaeggeler, K., Prevot, A. S., Dommen, J., Legreid, G., Reimann, S., and Baltensperger, U.: Residential wood burning in an Alpine valley as a source for oxygenated volatile organic compounds, hydrocarbons and organic acids, *Atmos. Environ.*, 42, 8278–8287, 2008. 1577

**Intercomparison of
ME-2 organic source
apportionment**

R. Fröhlich et al.

Title Page

Abstract

Introduction

Conclusions

References

Tables

Figures



Back

Close

Full Screen / Esc

Printer-friendly Version

Interactive Discussion



- Graus, M., Müller, M., and Hansel, A.: High resolution PTR-TOF: quantification and formula confirmation of VOC in real time, *J. Am. Soc. Mass Spectr.*, 21, 1037–1044, 2010. 1568
- Grieshop, A. P., Donahue, N. M., and Robinson, A. L.: Laboratory investigation of photochemical oxidation of organic aerosol from wood fires 2: analysis of aerosol mass spectrometer data, *Atmos. Chem. Phys.*, 9, 2227–2240, doi:10.5194/acp-9-2227-2009, 2009. 1577
- Hallquist, M., Wenger, J. C., Baltensperger, U., Rudich, Y., Simpson, D., Claeys, M., Dommen, J., Donahue, N. M., George, C., Goldstein, A. H., Hamilton, J. F., Herrmann, H., Hoffmann, T., Iinuma, Y., Jang, M., Jenkin, M. E., Jimenez, J. L., Kiendler-Scharr, A., Maenhaut, W., McFiggans, G., Mentel, Th. F., Monod, A., Prévôt, A. S. H., Seinfeld, J. H., Surratt, J. D., Szmigielski, R., and Wildt, J.: The formation, properties and impact of secondary organic aerosol: current and emerging issues, *Atmos. Chem. Phys.*, 9, 5155–5236, doi:10.5194/acp-9-5155-2009, 2009. 1563
- Hansel, A., Jordan, A., Holzinger, R., Prazeller, P., Vogel, W., and Lindinger, W.: Proton transfer reaction mass spectrometry: on-line trace gas analysis at the ppb level, *Int. J. Mass Spectrom.*, 149–150, 609–619, 1995. 1568
- Hansen, A., Rosen, H., and Novakov, T.: The aethalometer – an instrument for the real-time measurement of optical absorption by aerosol particles, *Sci. Total Environ.*, 36, 191–196, 1984. 1567
- Heringa, M. F., DeCarlo, P. F., Chirico, R., Tritscher, T., Dommen, J., Weingartner, E., Richter, R., Wehrle, G., Prévôt, A. S. H., and Baltensperger, U.: Investigations of primary and secondary particulate matter of different wood combustion appliances with a high-resolution time-of-flight aerosol mass spectrometer, *Atmos. Chem. Phys.*, 11, 5945–5957, doi:10.5194/acp-11-5945-2011, 2011. 1577
- Heringa, M. F., DeCarlo, P. F., Chirico, R., Lauber, A., Doberer, A., Good, J., Nussbaumer, T., Keller, A., Burtscher, H., Richard, A., Miljevic, B., Prevot, A. S. H., and Baltensperger, U.: Time-resolved characterization of primary emissions from residential wood combustion appliances, *Environ. Sci. Technol.*, 46, 11418–11425, doi:10.1021/es301654w, 2012. 1577
- Holzinger, R., Warneke, C., Hansel, A., Jordan, A., Lindinger, W., Scharffe, D. H., Schade, G., and Crutzen, P. J.: Biomass burning as a source of formaldehyde, acetaldehyde, methanol, acetone, acetonitrile, and hydrogen cyanide, *Geophys. Res. Lett.*, 26, 1161–1164, 1999. 1577

Intercomparison of ME-2 organic source apportionment

R. Fröhlich et al.

Title Page

Abstract

Introduction

Conclusions

References

Tables

Figures



Back

Close

Full Screen / Esc

Printer-friendly Version

Interactive Discussion



Hu, Q. H., Xie, Z. Q., Wang, X. M., Kang, H., and Zhang, P.: Levoglucosan indicates high levels of biomass burning aerosols over oceans from the Arctic to Antarctic, *Sci. Rep.*, 3, 3119, doi:10.1038/srep03119, 2013. 1577

Hu, W. W., Hu, M., Yuan, B., Jimenez, J. L., Tang, Q., Peng, J. F., Hu, W., Shao, M., Wang, M., Zeng, L. M., Wu, Y. S., Gong, Z. H., Huang, X. F., and He, L. Y.: Insights on organic aerosol aging and the influence of coal combustion at a regional receptor site of central eastern China, *Atmos. Chem. Phys.*, 13, 10095–10112, doi:10.5194/acp-13-10095-2013, 2013. 1563

Huang, R. J., Zhang, Y., Bozzetti, C., Ho, K. F., Cao, J. J., Han, Y., Daellenbach, K. R., Slowik, J. G., Platt, S. M., Canonaco, F., Zotter, P., Wolf, R., Pieber, S. M., Bruns, E. A., Crippa, M., Ciarelli, G., Piazzalunga, A., Schwikowski, M., Abbaszade, G., Schnelle-Kreis, J., Zimmermann, R., An, Z., Szidat, S., Baltensperger, U., El Haddad, I., and Prevot, A. S.: High secondary aerosol contribution to particulate pollution during haze events in China, *Nature*, 514, 218–222, 2014. 1563

Huffman, J. A., Jayne, J. T., Drewnick, F., Aiken, A. C., Onasch, T., Worsnop, D. R., and Jimenez, J. L.: Design, modeling, optimization, and experimental tests of a particle beam width probe for the Aerodyne aerosol mass spectrometer, *Aerosol Sci. Tech.*, 39, 1143–1163, doi:10.1080/02786820500423782, 2005. 1566

ISO13528: Statistical Methods for Use in Proficiency Testing by Interlaboratory Comparisons, ISO 13528, International Organization for Standardization, Geneva, Switzerland, 2005. 1587

Jacob, D. J., Field, B. D., Li, Q., Blake, D. R., de Gouw, J., Warneke, C., Hansel, A., Wisthaler, A., Singh, H. B., and Guenther, A.: Global budget of methanol: constraints from atmospheric observations, *J. Geophys. Res.-Atmos.*, 110, D08303, doi:10.1029/2004jd005172, 2005. 1577

Jayne, J., Leard, D., Zhang, X., Davidovits, P., Smith, K., Kolb, C., and Worsnop, D.: Development of an aerosol mass spectrometer for size and composition analysis of submicron particles, *Aerosol Sci. Tech.*, 33, 49–70, 2000. 1562

Jimenez, J. L., Canagaratna, M. R., Donahue, N. M., Prévôt, A. S. H., Zhang, Q., Kroll, J. H., DeCarlo, P. F., Allan, J. D., Coe, H., Ng, N. L., Aiken, A. C., Docherty, K. S., Ulbrich, I. M., Grieshop, A. P., Robinson, A. L., Duplissy, J., Smith, J. D., Wilson, K. R., Lanz, V. A., Hueglin, C., Sun, Y. L., Tian, J., Laaksonen, A., Raatikainen, T., Rautiainen, J., Vaattovaara, P., Ehn, M., Kulmala, M., Tomlinson, J. M., Collins, D. R., Cubison, M. J., E., Dunlea, J., Huffman, J. A., Onasch, T. B., Alfarra, M. R., Williams, P. I., Bower, K., Kondo, Y., Schneider, J., Drewnick, F., Borrmann, S., Weimer, S., Demerjian, K., Salcedo, D., Cottrell, L., Griffin, R., Takami, A., Miyoshi, T., Hatakeyama, S., Shimono, A., Sun, J. Y.,

**Intercomparison of
ME-2 organic source
apportionment**

R. Fröhlich et al.

Title Page

Abstract

Introduction

Conclusions

References

Tables

Figures



Back

Close

Full Screen / Esc

Printer-friendly Version

Interactive Discussion



- Zhang, Y. M., Dzepina, K., Kimmel, J. R., Sueper, D., Jayne, J. T., Herndon, S. C., Trimborn, A. M., Williams, L. R., Wood, E. C., Middlebrook, A. M., Kolb, C. E., Baltensperger, U., and Worsnop, D. R.: Evolution of organic aerosols in the atmosphere, *Science*, 326, 1525–1529, 2009. 1563
- 5 Kanakidou, M., Seinfeld, J. H., Pandis, S. N., Barnes, I., Dentener, F. J., Facchini, M. C., Van Dingenen, R., Ervens, B., Nenes, A., Nielsen, C. J., Swietlicki, E., Putaud, J. P., Balkanski, Y., Fuzzi, S., Horth, J., Moortgat, G. K., Winterhalter, R., Myhre, C. E. L., Tsigaridis, K., Vignati, E., Stephanou, E. G., and Wilson, J.: Organic aerosol and global climate modelling: a review, *Atmos. Chem. Phys.*, 5, 1053–1123, doi:10.5194/acp-5-1053-2005, 2005. 1562
- 10 Karagulian, F. and Belis, C. A.: Enhancing source apportionment with receptor models to foster the air quality directive implementation, *Int. J. Environ. Pollut.*, 50, 190–199, 2012. 1587
- Kimmel, J. R., Farmer, D. K., Cubison, M. J., Sueper, D., Tanner, C., Nemitz, E., Worsnop, D. R., Gonin, M., and Jimenez, J. L.: Real-time aerosol mass spectrometry with millisecond resolution, *Int. J. Mass Spectrom.*, 303, 15–26, 2011. 1574
- 15 Laden, F., Neas, L. M., Dockery, D. W., and Schwartz, J.: Association of fine particulate matter from different sources with daily mortality in six U.S. cities, *Environ. Health Persp.*, 108, 941–947, 2000. 1562
- Lanz, V. A., Alfara, M. R., Baltensperger, U., Buchmann, B., Hueglin, C., and Prévôt, A. S. H.: Source apportionment of submicron organic aerosols at an urban site by factor analytical modelling of aerosol mass spectra, *Atmos. Chem. Phys.*, 7, 1503–1522, doi:10.5194/acp-7-1503-2007, 2007. 1562
- 20 Lanz, V. A., Prévôt, A. S. H., Alfara, M. R., Weimer, S., Mohr, C., DeCarlo, P. F., Gianini, M. F. D., Hueglin, C., Schneider, J., Favez, O., D’Anna, B., George, C., and Baltensperger, U.: Characterization of aerosol chemical composition with aerosol mass spectrometry in Central Europe: an overview, *Atmos. Chem. Phys.*, 10, 10453–10471, doi:10.5194/acp-10-10453-2010, 2010. 1562, 1577
- 25 Li, Y. J., Lee, B. P., Su, L., Fung, J. C. H., and Chan, C.K.: Seasonal characteristics of fine particulate matter (PM) based on high-resolution time-of-flight aerosol mass spectrometric (HR-ToF-AMS) measurements at the HKUST Supersite in Hong Kong, *Atmos. Chem. Phys.*, 15, 37–53, doi:10.5194/acp-15-37-2015, 2015. 1575
- 30 Lim, S. S., Vos, T., Flaxman, A. D., Danaei, G., Shibuya, K., Adair-Rohani, H., AlMazroa, M. A., Amann, M., Anderson, H. R., Andrews, K. G., Aryee, M., Atkinson, C., Bacchus, L. J., Bahalim, A. N., Balakrishnan, K., Balmes, J., Barker-Collo, S., Baxter, A., Bell, M. L., Blore, J. D.,

Intercomparison of ME-2 organic source apportionment

R. Fröhlich et al.

Title Page

Abstract

Introduction

Conclusions

References

Tables

Figures



Back

Close

Full Screen / Esc

Printer-friendly Version

Interactive Discussion



Blyth, F., Bonner, C., Borges, G., Bourne, R., Boussinesq, M., Brauer, M., Brooks, P., Bruce, N. G., Brunekreef, B., Bryan-Hancock, C., Bucello, C., Buchbinder, R., Bull, F., Burnett, R. T., Byers, T. E., Calabria, B., Carapetis, J., Carnahan, E., Chafe, Z., Charlson, F., Chen, H., Chen, J. S., Cheng, A. T.-A., Child, J. C., Cohen, A., Colson, K. E., Cowie, B. C., Darby, S., Darling, S., Davis, A., Degenhardt, L., Dentener, F., Jarlais, D. C. D., Devries, K., Dherani, M., Ding, E. L., Dorsey, E. R., Driscoll, T., Edmond, K., Ali, S. E., Engell, R. E., Erwin, P. J., Fahimi, S., Falder, G., Farzadfar, F., Ferrari, A., Finucane, M. M., Flaxman, S., Fowkes, F. G. R., Freedman, G., Freeman, M. K., Gakidou, E., Ghosh, S., Giovannucci, E., Gmel, G., Graham, K., Grainger, R., Grant, B., Gunnell, D., Gutierrez, H. R., Hall, W., Hoek, H. W., Hogan, A., Hosgood III, H. D., Hoy, D., Hu, H., Hubbell, B. J., Hutchings, S. J., Ibeanusi, S. E., Jacklyn, G. L., Jasrasaria, R., Jonas, J. B., Kan, H., Kanis, J. A., Kassebaum, N., Kawakami, N., Khang, Y.-H., Khatibzadeh, S., Khoo, J.-P., Kok, C., Laden, F., Lalloo, R., Lan, Q., Lathlean, T., Leasher, J. L., Leigh, J., Li, Y., Lin, J. K., Lipshultz, S. E., London, S., Lozano, R., Lu, Y., Mak, J., Malekzadeh, R., Mallinger, L., Marcenes, W., March, L., Marks, R., Martin, R., McGale, P., McGrath, J., Mehta, S., Memish, Z. A., Mensah, G. A., Merriman, T. R., Micha, R., Michaud, C., Mishra, V., Hanafiah, K. M., Mokdad, A. A., Morawska, L., Mozaffarian, D., Murphy, T., Naghavi, M., Neal, B., Nelson, P. K., Nolla, J. M., Norman, R., Olives, C., Omer, S. B., Orchard, J., Osborne, R., Ostro, B., Page, A., Pandey, K. D., Parry, C. D., Passmore, E., Patra, J., Pearce, N., Pelizzari, P. M., Petzold, M., Phillips, M. R., Pope, D., Pope III, C. A., Powles, J., Rao, M., Razavi, H., Rehfues, E. A., Rehm, J. T., Ritz, B., Rivara, F. P., Roberts, T., Robinson, C., Rodriguez-Portales, J. A., Romieu, I., Room, R., Rosenfeld, L. C., Roy, A., Rushton, L., Salomon, J. A., Sampson, U., Sanchez-Riera, L., Sanman, E., Sapkota, A., Seedat, S., Shi, P., Shield, K., Shivakoti, R., Singh, G. M., Sleet, D. A., Smith, E., Smith, K. R., Stapelberg, N. J., Steenland, K., Stöckl, H., Stovner, L. J., Straif, K., Straney, L., Thurston, G. D., Tran, J. H., Dingenen, R. V., van Donkelaar, A., Veerman, J. L., Vijayakumar, L., Weintraub, R., Weissman, M. M., White, R. A., Whiteford, H., Wiersma, S. T., Wilkinson, J. D., Williams, H. C., Williams, W., Wilson, N., Woolf, A. D., Yip, P., Zielinski, J. M., Lopez, A. D., Murray, C. J., and Ezzati, M.: A comparative risk assessment of burden of disease and injury attributable to 67 risk factors and risk factor clusters in 21 regions, 1990–2010: a systematic analysis for the Global Burden of Disease Study 2010, *Lancet*, 380, 2224–2260, 2013. 1562

Liu, D., Allan, J. D., Young, D. E., Coe, H., Beddows, D., Fleming, Z. L., Flynn, M. J., Gallagher, M. W., Harrison, R. M., Lee, J., Prevot, A. S. H., Taylor, J. W., Yin, J., Williams, P. I., and

**Intercomparison of
ME-2 organic source
apportionment**

R. Fröhlich et al.

Title Page

Abstract

Introduction

Conclusions

References

Tables

Figures



Back

Close

Full Screen / Esc

Printer-friendly Version

Interactive Discussion



Zotter, P.: Size distribution, mixing state and source apportionment of black carbon aerosol in London during wintertime, *Atmos. Chem. Phys.*, 14, 10061–10084, doi:10.5194/acp-14-10061-2014, 2014. 1568

Liu, P., Ziemann, P. J., Kittelson, D. B., and McMurry, P. H.: Generating particle beams of controlled dimensions and divergence: II. experimental evaluation of particle motion in aerodynamic lenses and nozzle expansions, *Aerosol Sci. Tech.*, 22, 314–324, 1995a. 1565

Liu, P., Ziemann, P. J., Kittelson, D. B., and McMurry, P. H.: Generating particle beams of controlled dimensions and divergence: I. theory of particle motion in aerodynamic lenses and nozzle expansions, *Aerosol Sci. Tech.*, 22, 293–313, 1995b. 1565

Liu, P. S. K., Deng, R., Smith, K. A., Williams, L. R., Jayne, J. T., Canagaratna, M. R., Moore, K., Onasch, T. B., Worsnop, D. R., and Deshler, T.: Transmission efficiency of an aerodynamic focusing lens system: comparison of model calculations and laboratory measurements for the Aerodyne aerosol mass spectrometer, *Aerosol Sci. Tech.*, 41, 721–733, 2007. 1565

Lohmann, U. and Feichter, J.: Global indirect aerosol effects: a review, *Atmos. Chem. Phys.*, 5, 715–737, doi:10.5194/acp-5-715-2005, 2005. 1562

Mahowald, N.: Aerosol indirect effect on biogeochemical cycles and climate, *Science*, 334, 794–796, 2011. 1562

Mathers, C. D., Fat, D. M., Inoue, M., Rao, C., and Lopez, A. D.: Counting the dead and what they died from: an assessment of the global status of cause of death data, *B. World Health Organ.*, 83, 171–177, 2005. 1562

Matthew, B. M., Middlebrook, A. M., and Onasch, T. B.: Collection efficiencies in an Aerodyne aerosol mass spectrometer as a function of particle phase for laboratory generated aerosols, *Aerosol Sci. Tech.*, 42, 884–898, 2008. 1566

Mercado, L. M., Bellouin, N., Sitch, S., Boucher, O., Huntingford, C., Wild, M., and Cox, P. M.: Impact of changes in diffuse radiation on the global land carbon sink, *Nature*, 458, 1014–1017, 2009. 1562

Mohr, C., Huffman, J. A., Cubison, M. J., Aiken, A. C., Docherty, K. S., Kimmel, J. R., Ulbrich, I. M., Hannigan, M., and Jimenez, J. L.: Characterization of primary organic aerosol emissions from meat cooking, trash burning, and motor vehicles with high-resolution aerosol mass spectrometry and comparison with ambient and chamber observations, *Environ. Sci. Technol.*, 43, 2443–2449, doi:10.1021/es8011518, 2009. 1569

Mohr, C., DeCarlo, P. F., Heringa, M. F., Chirico, R., Slowik, J. G., Richter, R., Reche, C., Alastuey, A., Querol, X., Seco, R., Peñuelas, J., Jiménez, J. L., Crippa, M., Zimmermann, R.,

Intercomparison of ME-2 organic source apportionment

R. Fröhlich et al.

Title Page

Abstract

Introduction

Conclusions

References

Tables

Figures



Back

Close

Full Screen / Esc

Printer-friendly Version

Interactive Discussion



Baltensperger, U., and Prévôt, A. S. H.: Identification and quantification of organic aerosol from cooking and other sources in Barcelona using aerosol mass spectrometer data, *Atmos. Chem. Phys.*, 12, 1649–1665, doi:10.5194/acp-12-1649-2012, 2012. 1563, 1576

5 Ng, N. L., Canagaratna, M. R., Zhang, Q., Jimenez, J. L., Tian, J., Ulbrich, I. M., Kroll, J. H., Docherty, K. S., Chhabra, P. S., Bahreini, R., Murphy, S. M., Seinfeld, J. H., Hildebrandt, L., Donahue, N. M., DeCarlo, P. F., Lanz, V. A., Prévôt, A. S. H., Dinar, E., Rudich, Y., and Worsnop, D. R.: Organic aerosol components observed in Northern Hemispheric datasets from Aerosol Mass Spectrometry, *Atmos. Chem. Phys.*, 10, 4625–4641, doi:10.5194/acp-10-4625-2010, 2010. 1563, 1572, 1573, 1574

10 Ng, N. L., Canagaratna, M. R., Jimenez, J. L., Chhabra, P. S., Seinfeld, J. H., and Worsnop, D. R.: Changes in organic aerosol composition with aging inferred from aerosol mass spectra, *Atmos. Chem. Phys.*, 11, 6465–6474, doi:10.5194/acp-11-6465-2011, 2011a. 1573

15 Ng, N. L., Canagaratna, M. R., Jimenez, J. L., Zhang, Q., Ulbrich, I. M., and Worsnop, D. R.: Real-time methods for estimating organic component mass concentrations from aerosol mass spectrometer data, *Environ. Sci. Technol.*, 45, 910–916, doi:10.1021/es102951k, 2011b. 1568, 1585

20 Ng, N. L., Herndon, S. C., Trimborn, A., Canagaratna, M. R., Croteau, P. L., Onasch, T. B., Sueper, D., Worsnop, D. R., Zhang, Q., Sun, Y. L., and Jayne, J. T.: An aerosol chemical speciation monitor (ACSM) for routine monitoring of the composition and mass concentrations of ambient aerosol, *Aerosol Sci. Tech.*, 45, 780–794, 2011c. 1562, 1570, 1574

25 Ovadnevaite, J., Ceburnis, D., Canagaratna, M., Berresheim, H., Bialek, J., Martucci, G., Worsnop, D. R., and O'Dowd, C.: On the effect of wind speed on submicron sea salt mass concentrations and source fluxes, *J. Geophys. Res.-Atmos.*, 117, D16201, doi:10.1029/2011jd017379, 2012. 1572

Paatero, P.: Least squares formulation of robust non-negative factor analysis, *Chemometr. Intell. Lab.*, 37, 23–35, 1997. 1562, 1568, 1570

Paatero, P.: The multilinear engine – a table-driven, least squares program for solving multilinear problems, including the n-way parallel factor analysis model, *J. Comput. Graph. Stat.*, 8, 854–888, 1999. 1562

30 Paatero, P. and Hopke, P. K.: Rotational tools for factor analytic models, *J. Chemometr.*, 23, 91–100, 2009. 1569

**Intercomparison of
ME-2 organic source
apportionment**

R. Fröhlich et al.

Title Page

Abstract

Introduction

Conclusions

References

Tables

Figures



Back

Close

Full Screen / Esc

Printer-friendly Version

Interactive Discussion



- Paatero, P. and Tapper, U.: Positive matrix factorization: a non-negative factor model with optimal utilization of error estimates of data values, *Environmetrics*, 5, 111–126, 1994. 1562, 1568
- Paatero, P., Eberly, S., Brown, S. G., and Norris, G. A.: Methods for estimating uncertainty in factor analytic solutions, *Atmos. Meas. Tech.*, 7, 781–797, doi:10.5194/amt-7-781-2014, 2014. 1563
- Petit, J.-E., Favez, O., Sciare, J., Crenn, V., Sarda-Estève, R., Bonnaire, N., Močnik, G., Dupont, J.-C., Haefelin, M., and Leoz-Garziandia, E.: Two years of near real-time chemical composition of submicron aerosols in the region of Paris using an Aerosol Chemical Specification Monitor (ACSm) and a multi-wavelength Aethalometer, *Atmos. Chem. Phys. Discuss.*, 14, 24221–24271, doi:10.5194/acpd-14-24221-2014, 2014. 1572
- Pope, C. A. and Dockery, D. W.: Health effects of fine particulate air pollution: lines that connect, *J. Air Waste Manage.*, 56, 709–742, 2006. 1562
- Saleh, R., Hennigan, C. J., McMeeking, G. R., Chuang, W. K., Robinson, E. S., Coe, H., Donahue, N. M., and Robinson, A. L.: Absorptivity of brown carbon in fresh and photo-chemically aged biomass-burning emissions, *Atmos. Chem. Phys.*, 13, 7683–7693, doi:10.5194/acp-13-7683-2013, 2013. 1568
- Sandradewi, J., Prévôt, A. S., Szidat, S., Perron, N., Alfarra, M. R., Lanz, V. A., Weingartner, E., and Baltensperger, U.: Using aerosol light absorption measurements for the quantitative determination of wood burning and traffic emission contributions to particulate matter, *Environ. Sci. Technol.*, 42, 3316–3323, 2008. 1567, 1568
- Sciare, J., d'Argouges, O., Sarda-Estève, R., Gaimoz, C., Dolgorouky, C., Bonnaire, N., Favez, O., Bonsang, B., and Gros, V.: Large contribution of water-insoluble secondary organic aerosols in the region of Paris (France) during wintertime, *J. Geophys. Res.-Atmos.*, 116, D22203, doi:10.1029/2011jd015756, 2011. 1568
- Seaton, A., Godden, D., MacNee, W., and Donaldson, K.: Particulate air pollution and acute health effects, *Lancet*, 345, 176–178, 1995. 1562
- Simoneit, B., Schauer, J., Nolte, C., Oros, D., Elias, V., Fraser, M., Rogge, W., and Cass, G.: Levoglucosan, a tracer for cellulose in biomass burning and atmospheric particles, *Atmos. Environ.*, 33, 173–182, 1999. 1577
- Slowik, J. G., Vlasenko, A., McGuire, M., Evans, G. J., and Abbatt, J. P. D.: Simultaneous factor analysis of organic particle and gas mass spectra: AMS and PTR-MS measurements at

**Intercomparison of
ME-2 organic source
apportionment**

R. Fröhlich et al.

Title Page

Abstract

Introduction

Conclusions

References

Tables

Figures



Back

Close

Full Screen / Esc

Printer-friendly Version

Interactive Discussion



an urban site, *Atmos. Chem. Phys.*, 10, 1969–1988, doi:10.5194/acp-10-1969-2010, 2010. 1563, 1576

Stevens, B. and Feingold, G.: Untangling aerosol effects on clouds and precipitation in a buffered system, *Nature*, 461, 607–613, 2009. 1562

5 Sun, J., Zhang, Q., Canagaratna, M. R., Zhang, Y., Ng, N. L., Sun, Y., Jayne, J. T., Zhang, X., Zhang, X., and Worsnop, D. R.: Highly time- and size-resolved characterization of submicron aerosol particles in Beijing using an Aerodyne aerosol mass spectrometer, *Atmos. Environ.*, 44, 131–140, 2010. 1569

10 Sun, Y.-L., Zhang, Q., Schwab, J. J., Demerjian, K. L., Chen, W.-N., Bae, M.-S., Hung, H.-M., Hogrefe, O., Frank, B., Rattigan, O. V., and Lin, Y.-C.: Characterization of the sources and processes of organic and inorganic aerosols in New York city with a high-resolution time-of-flight aerosol mass spectrometer, *Atmos. Chem. Phys.*, 11, 1581–1602, doi:10.5194/acp-11-1581-2011, 2011. 1563, 1576

15 Timonen, H., Carbone, S., Aurela, M., Saarnio, K., Saarikoski, S., Ng, N. L., Canagaratna, M. R., Kulmala, M., Kerminen, V.-M., Worsnop, D. R., and Hillamo, R.: Characteristics, sources and water-solubility of ambient submicron organic aerosol in springtime in Helsinki, Finland, *J. Aerosol Sci.*, 56, 61–77, 2013. 1563

20 Ulbrich, I. M., Canagaratna, M. R., Zhang, Q., Worsnop, D. R., and Jimenez, J. L.: Interpretation of organic components from Positive Matrix Factorization of aerosol mass spectrometric data, *Atmos. Chem. Phys.*, 9, 2891–2918, doi:10.5194/acp-9-2891-2009, 2009. 1562, 1571, 1587

Wang, Y., Wang, M., Zhang, R., Ghan, S. J., Lin, Y., Hu, J., Pan, B., Levy, M., Jiang, J. H., and Molina, M. J.: Assessing the effects of anthropogenic aerosols on Pacific storm track using a multiscale global climate model, *P. Natl. Acad. Sci. USA*, 111, 6894–6899, 2014a. 1562

25 Wang, Y., Zhang, R., and Saravanan, R.: Asian pollution climatically modulates mid-latitude cyclones following hierarchical modelling and observational analysis, *Nat. Commun.*, 5, 3098, doi:10.1038/ncomms4098, 2014b. 1562

30 Watson, J. G., Robinson, N. F., Lewis, C., Coulter, T., Chow, J. C., Fujita, E. M., Lowenthal, D., Conner, T. L., Henry, R. C., and Willis, R. D.: Chemical Mass Balance Receptor Model Version 8 (CMB8) User's Manual, Prepared for US Environmental Protection Agency, Research Triangle Park, NC, by Desert Research Institute, Reno, NV, 1997. 1568

Weimer, S., Alfara, M. R., Schreiber, D., Mohr, M., Prévôt, A. S. H., and Baltensperger, U.: Organic aerosol mass spectral signatures from wood-burning emissions:

influence of burning conditions and wood type, *J. Geophys. Res.-Atmos.*, 113, D10304, doi:10.1029/2007jd009309, 2008. 1577

Zhang, Q., Alfarra, M. R., Worsnop, D. R., Allan, J. D., Coe, H., Canagaratna, M. R., and Jimenez, J. L.: Deconvolution and quantification of hydrocarbon-like and oxygenated organic aerosols based on aerosol mass spectrometry, *Environ. Sci. Technol.*, 39, 4938–4952, doi:10.1021/es048568l, 2005a. 1563

Zhang, Q., Worsnop, D. R., Canagaratna, M. R., and Jimenez, J. L.: Hydrocarbon-like and oxygenated organic aerosols in Pittsburgh: insights into sources and processes of organic aerosols, *Atmos. Chem. Phys.*, 5, 3289–3311, doi:10.5194/acp-5-3289-2005, 2005b. 1563, 1576

Zhang, Q., Jimenez, J. L., Canagaratna, M. R., Ulbrich, I. M., Ng, N. L., Worsnop, D. R., and Sun, Y.: Understanding atmospheric organic aerosols via factor analysis of aerosol mass spectrometry: a review, *Anal. Bioanal. Chem.*, 401, 3045–3067, 2011. 1563, 1568, 1575, 1577

Zhang, X., Smith, K. A., Worsnop, D. R., Jimenez, J. L., Jayne, J. T., Kolb, C. E., Morris, J., and Davidovits, P.: Numerical characterization of particle beam collimation: part II integrated aerodynamic-lens–nozzle system, *Aerosol Sci. Tech.*, 38, 619–638, 2004. 1565

AMTD

8, 1559–1613, 2015

Intercomparison of ME-2 organic source apportionment

R. Fröhlich et al.

Title Page

Abstract

Introduction

Conclusions

References

Tables

Figures



Back

Close

Full Screen / Esc

Printer-friendly Version

Interactive Discussion



Intercomparison of ME-2 organic source apportionment

R. Fröhlich et al.

Table 1. *a* values of the best solutions for each instrument. Anchors used in the ME-2 analysis: HOA anchor left table column: individual reference spectra from previous pure PMF solution of the same data set (HOA_{indv}), right table column: $\text{HOA}_{\text{Paris}}$, COA anchors left and right table columns: $\text{COA}_{\text{Paris}}$. In some cases (#2, 3, 4 and 12) the time series correlation with external tracers was better (higher R^2) without constraint of the HOA profile.

<i>a</i> value	$\text{HOA}_{\text{indv}} / \text{COA}_{\text{Paris}}$	$\text{HOA}_{\text{Paris}} / \text{COA}_{\text{Paris}}$
ToF	0.05/0.05	0.10/0.10
#1	0.05/0.05	0.35/0.05
#2	free/0.04	0.25/0.15
#3	free/0.10	0.20/0.10
#4	free/0.15	0.15/0.15
#5	0.05/0.15	0.45/0.25
#6	0.05/0.05	0.30/0.30
#7	0.05/0.05	0.05/0.25
#8	0.05/0.05	0.20/0.15
#9	0.10/0.10	0.35/0.05
#10	0.04/0.20	0.20/0.20
#11	0.01/0.04	0.10/0.05
#12	free/0.10	0.20/0.30
#13	0.05/0.05	0.60/0.05

Title Page

Abstract

Introduction

Conclusions

References

Tables

Figures

◀

▶

◀

▶

Back

Close

Full Screen / Esc

Printer-friendly Version

Interactive Discussion



Intercomparison of ME-2 organic source apportionment

R. Fröhlich et al.

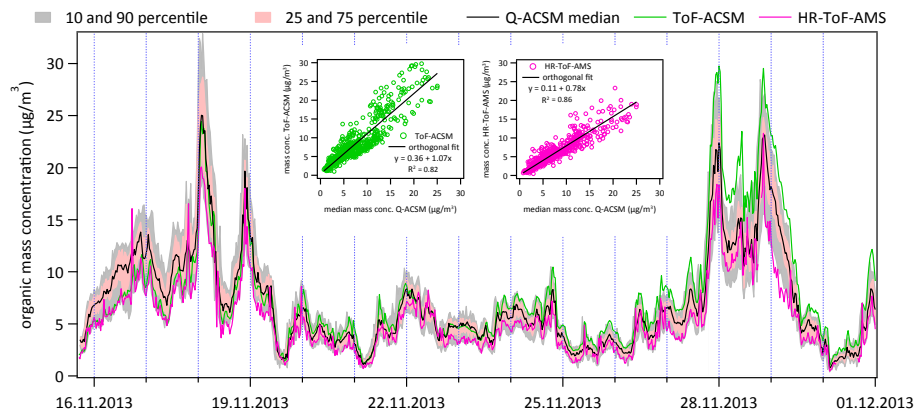


Figure 1. Time series of bulk organic matter for all 15 instruments in $\mu\text{g m}^{-3}$ ($\text{CE} = 0.5$, $\text{RIE}_{\text{org}} = 1.4$). The green trace shows organic matter measured by the ToF-ACSM, the pink trace HR-ToF-AMS organic matter and the black trace the median of organic matter measured by the 13 Q-ACSMs. Since all ACSMs run with slightly different time steps all data shown in this plot had to be re-gridded to the same 30 min time scale for the calculation of median and inter-percentile ranges. The light red and light grey regions indicate the 25–75 percentile range and the 10–90 percentile range of the Q-ACSM measurements, respectively. The two small insets show the correlation between ToF-ACSM and median Q-ACSM organic (green) and the same for HR-ToF-AMS and median Q-ACSM (pink). Slopes and coefficients of determination of an orthogonal distance regression are given in the plots. Average organic matter concentrations during the whole period were $6.9 \mu\text{g m}^{-3}$.

Title Page

Abstract

Introduction

Conclusions

References

Tables

Figures

◀

▶

◀

▶

Back

Close

Full Screen / Esc

Printer-friendly Version

Interactive Discussion



Intercomparison of
ME-2 organic source
apportionment

R. Fröhlich et al.

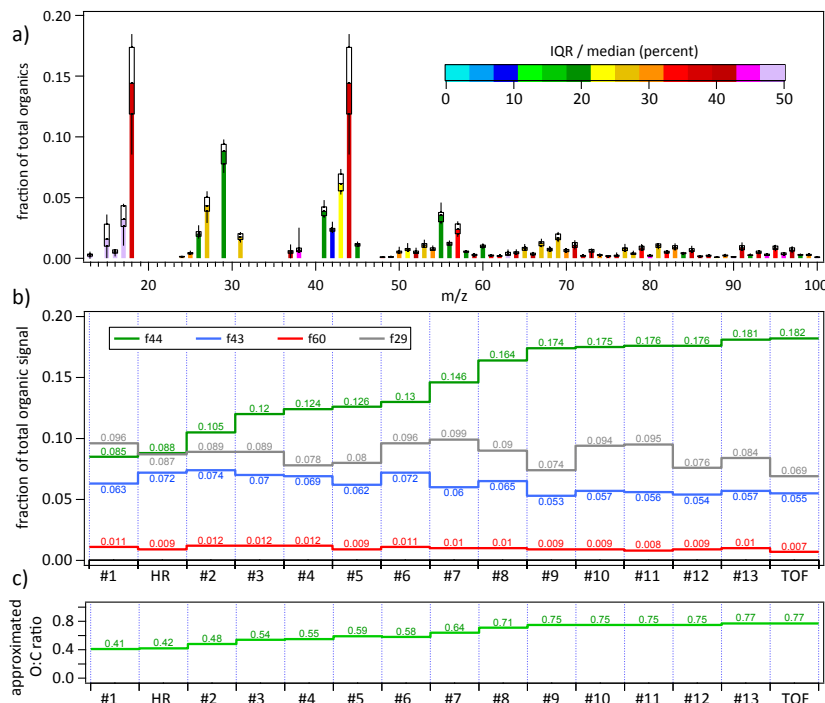


Figure 2. (a) Median organic mass spectrum of the 13 Q-ACSMs (sticks) during interruption-free 20 h period (average of ~ 1200 mass spectra). The boxes represent the IQR for each m/z stick and the whiskers represent the corresponding full range over all instruments. The line in the box indicates the median. The colour bar represents the ratio of the width of the individual boxes in relation to the corresponding median in percent. (b) Fractions of the total organic signal at single m/z channels for all 15 participating instruments sorted by fraction of m/z 44. Gray: f29, blue: f43, green: f44, red: f60. The respective fractions are given as numbers in the same colours. (c) O:C ratio calculated via the formula given in Aiken et al. (2008) for all 15 participating instruments sorted by f44. O:C values are also given as numbers.

Intercomparison of
ME-2 organic source
apportionment

R. Fröhlich et al.

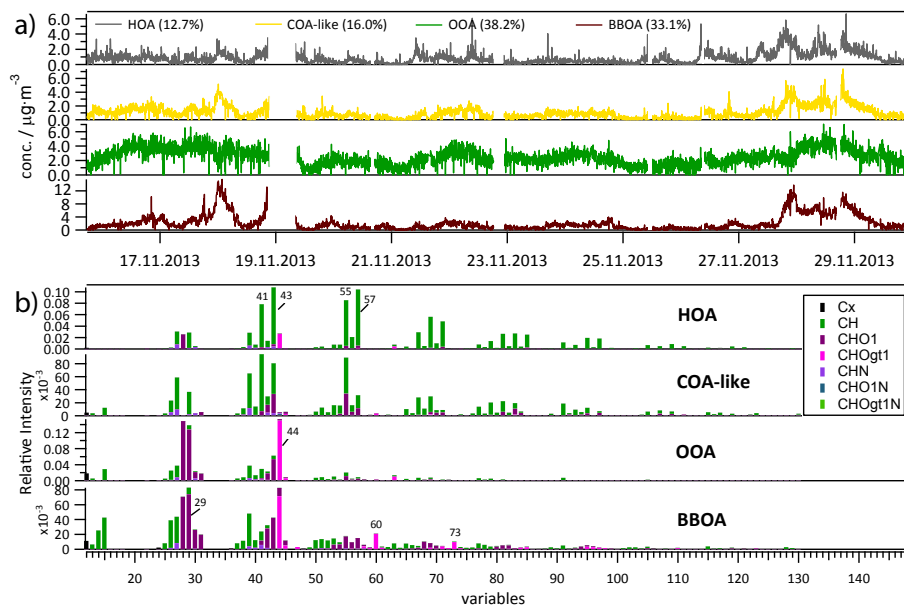


Figure 3. Factor time series in $\mu\text{g}\cdot\text{m}^{-3}$ **(a)** and relative factor profiles **(b)** of the HR PMF source apportionment. In both **(a)** and **(b)** the factors are ordered from top to down as follows: HOA (grey), COA-like (yellow), OOA (green), BBOA (brown). Average contributions of each factor are given in brackets in **(a)**. The profiles are shown on a UMR axis with different colours for the various species families (see legend in the plot, gt here means “greater than”).

Title Page

Abstract

Introduction

Conclusions

References

Tables

Figures



Back

Close

Full Screen / Esc

Printer-friendly Version

Interactive Discussion



Intercomparison of ME-2 organic source apportionment

R. Fröhlich et al.

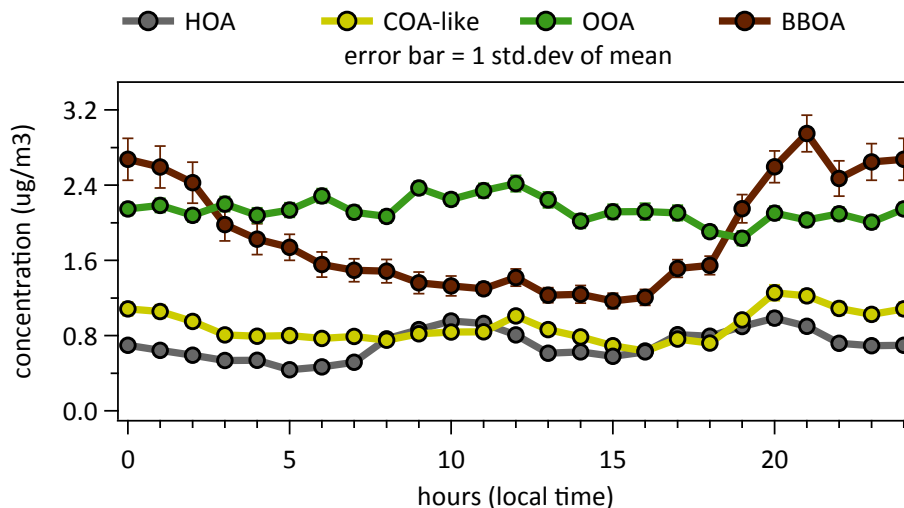


Figure 4. Diurnal variation (local time) of absolute factor concentrations in $\mu\text{g m}^{-3}$ ($\text{CE} = 0.5$, $\text{RIE}_{\text{org}} = 1.4$). Gray: HOA, yellow: COA-like, green: OOA, brown: BBOA. The error bars represent the first SD. In some cases (e.g. HOA) the error bars are not visible because they are smaller than the marker size.

Intercomparison of
ME-2 organic source
apportionment

R. Fröhlich et al.

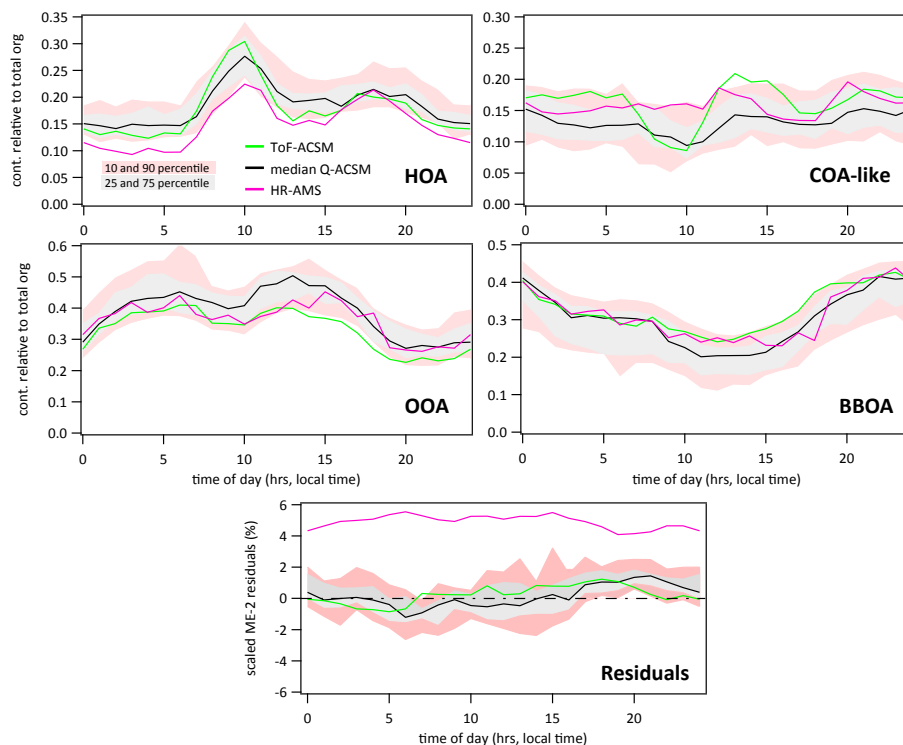


Figure 5. Diurnal variation of the four source factors and PMF residuals. The upper four panels display the relative contribution of the respective sources to the total apportioned organic matter. Top left: HOA, top right: COA-like, bottom left: OOA, bottom right: BBOA. Green trace: ToF-ACSM, pink trace: HR-ToF-AMS, black trace: median of all 13 Q-ACSMs. The IQR and the 10–90 percentile range of the Q-ACSMs are indicated as light grey and light red regions, respectively. The lower panel shows the residual organic concentration not explained by the presented solution in % of the total organic concentration. The time is local time (UTC + 1).

Intercomparison of
ME-2 organic source
apportionment

R. Fröhlich et al.

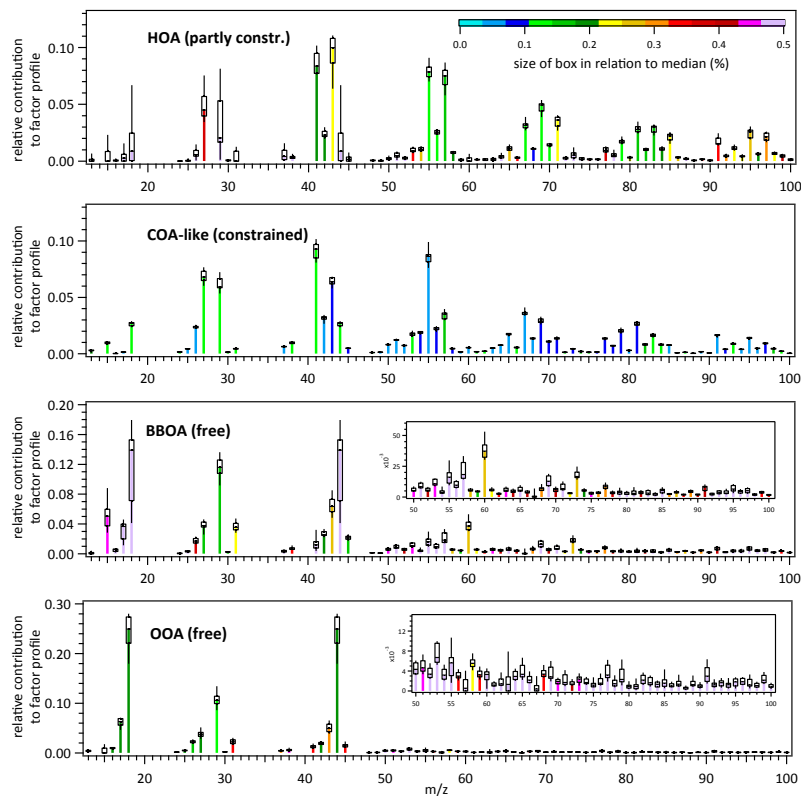


Figure 6. Median source factor profiles of the 13 Q-ACSMs (sticks) sorted from top to bottom as follows: HOA, COA-like, BBOA, OOA. The boxes represent the IQR for each m/z stick and the whiskers represent the corresponding full range over all instruments. The line in the box indicates the median. The colour bar represents the ratio of the width of the individual boxes in relation to the corresponding median in percent. The region between m/z 50 and 100 is enlarged in the two small insets for the BBOA and the OOA factor.

[Title Page](#)[Abstract](#)[Introduction](#)[Conclusions](#)[References](#)[Tables](#)[Figures](#)[Back](#)[Close](#)[Full Screen / Esc](#)[Printer-friendly Version](#)[Interactive Discussion](#)

Intercomparison of
ME-2 organic source
apportionment

R. Fröhlich et al.

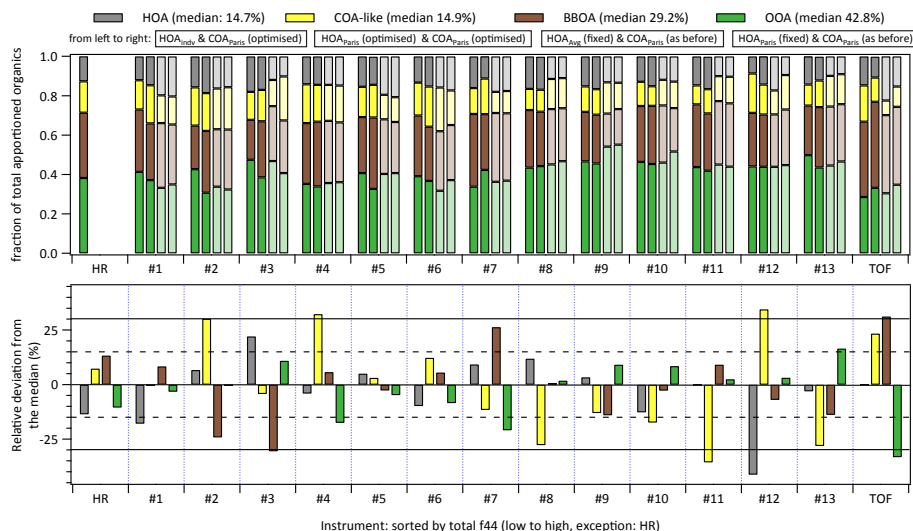


Figure 7. (Top) Relative factor contributions of HOA (grey), COA-like (yellow), OOA (green) and BBOA (brown) for each of the 15 participating instruments sorted by f44 in the corresponding total organic spectrum (low to high). Each time four bar plots are shown. Fully coloured: a values were optimised, lightly coloured: $a_{\text{HOA}} = 0$ and a_{COA} equal to value in the second fully coloured bar from the left (cf. Table 1). For each of the left-most bar plots HOA was either fully unconstrained or HOA_{indv} extracted from a previous pure PMF solution of the same data set. For the second bar the anchors $\text{HOA}_{\text{Paris}}$ and $\text{COA}_{\text{Paris}}$ were used and optimised in each case. For the third and fourth bar from the left $\text{COA}_{\text{Paris}}$ was used as anchor with the same a values as before while $a_{\text{HOA}} = 0$. Different HOA anchors were used in the third (HOA_{Avg}) and the fourth ($\text{HOA}_{\text{Paris}}$) bars from the left. Median values of the left-most solutions are given in brackets in the legend. (Bottom) Relative deviation from the median in percent of each factor in each of the 15 instruments sorted by total f44 (low to high). The solid line confines the $\pm 30\%$ region and the dashed line the $\pm 15\%$ region. Colours are the same as in the top panel.

Title Page

Abstract

Introduction

Conclusions

References

Tables

Figures



Back

Close

Full Screen / Esc

Printer-friendly Version

Interactive Discussion

